Türkiye Jeoloji Bülteni
Geological Bulletin of Turkey
69 (2026) 121-168
doi:10.25288/tjb.1765110

Facies Evolution and Lake-Type Variability Related to Climatic Cycles in the Late Triassic Çakrazboz Formation, Western Pontides, Türkiye

Geç Triyas Yaşlı Çakrazboz Formasyonu'nda Fasiyes Evrimi ve İklimsel Döngülere Bağlı Göl Tipi Değişkenliği, Batı Pontidler, Türkiye

Gül Şen[1, *], İsmail Ömer Yılmaz[2]

[1] Van Yüzüncü Yıl Üniversitesi, Mühendislik Fakültesi, Jeoloji Mühendisliği Bölümü, 65080, Tuşba, Van, Türkiye
[2] Orta Doğu Teknik Üniversitesi, Mühendislik Fakültesi Jeoloji Mühendisliği Bölümü, 06800, Çankaya, Ankara, Türkiye

• Geliş/Received: 16.08.2025 • Düzeltilmiş Metin Geliş/Revised Manuscript Received: 24.11.2025 • Kabul/Accepted: 07.12.2025
• Çevrimiçi Yayın/Available online: 13.01.2026 • Baskı/Printed: 31.01.2026

Araştırma Makalesi/Research Article *Türkiye Jeol. Bül. / Geol. Bull. Turkey*

Abstract: The Çakrazboz Formation, located in the Amasra–Kastamonu region of the Western Pontides (NW Türkiye), represents the only known Triassic continental sedimentary succession in Türkiye. This study integrates sedimentological, petrographic, and stratigraphic data from six measured sections to reconstruct depositional environments and evaluate paleoclimatic controls. Field and thin-section analyses reveal a complex facies mosaic comprising three major lithofacies groups: lacustrine, palustrine, and fluvial. Lacustrine facies are represented by carbonate-rich successions, including micrite, wackestone, and packstone, indicating low-energy profundal to sublittoral settings. Palustrine facies, occurring predominantly in marginal lake environments, are characterized by pedogenic overprinting, fenestral fabrics, root traces, and desiccation features, with the Bozköy and Başköy-1 sections showing more pronounced development of these features. Başköy-2 and Başköy-3 exhibit fluvial point-bar deposits with upward-fining successions and pedogenically modified mudstones, representing meandering river systems deposited during overfilled lake stages. Stratigraphic and sedimentological evidence indicates that the basin experienced repeated shifts between underfilled, balanced-fill, and overfilled lake stages. Carbonate-rich successions in the Çakrazboz and lower İncigez sections represent low-energy profundal lacustrine conditions typical of underfilled stages. The upper İncigez and Başköy-1 sections preserve features of balanced-fill conditions, with fining-upward transgressive intervals overlain by progradational littoral facies. Overfilled conditions are locally recorded in Bozköy and in the upper parts of Başköy-1, as evidenced by laterally extensive successions that thicken and coarsen upward, reflecting sustained freshwater inflow. These vertical facies transitions, stacking patterns, and diagenetic overprints are indicative of orbitally forced lake-level fluctuations under subhumid to semi-arid climate regimes, contributing to a broader understanding of Late Triassic continental basin evolution, facies architecture, and climate-controlled sedimentation.

Keywords: Çakrazboz Formation, facies evolution, lake-type variability, orbital cycles, oaleoclimate, Western Pontides

Öz: *Çakrazboz Formasyonu, Türkiye'de bilinen tek Triyas yaşlı kıtasal tortul istif olarak Batı Pontidler'in (Kuzeybatı Türkiye) Amasra–Kastamonu yöresinde yüzeylenmektedir. Bu çalışmada, altı stratigrafik kesitten elde edilen sedimantolojik, petrografik ve stratigrafik veriler birleştirilerek depolanma ortamları yeniden yapılandırılmış ve paleoiklimsel kontrol mekanizmaları değerlendirilmiştir. Saha ve ince kesit analizleri, üç ana litofasiyes grubundan*

Correspondence / *Yazışma:* gul.sen@yyu.edu.tr

oluşan karmaşık bir fasiyes mozaiğini ortaya koymaktadır: göl, bataklık (palustrin) ve akarsu (flüviyal). Gölsel istifler, çamurtaşı (mikrit), vaketaşı ve tanetaşı gibi karbonatça zengin fasiyeslerden oluşmakta ve düşük enerjili derin göl-sublitoral (profundal–sublittoral) ortamlara işaret etmektedir. Palustrin fasiyesler, göl kenarı ortamlarında yaygın olup pedojenik alterasyon, fenestral dokular, kök izleri ve kuruma çatlakları ile karakterizedir; Bozköy ve Başköy-1 kesitlerinde bu özellikler daha belirgin şekilde gelişmiştir. Başköy-2 ve Başköy-3 kesitleri, yukarıya doğru incelen kumtaşı-çamurtaşı ardalanmaları ve pedojeneze uğramış çamurtaşlarından oluşan menderesli akarsu sistemlerine ait nokta bar istiflerini içerir ve bu istifler, gölün aşırı dolduğu (overfilled) evrelerde çökelmiştir. Stratigrafik ve sedimantolojik veriler, havzanın tekrar eden şekilde yetersiz dolu (underfilled), dengeli dolu (balanced-fill) ve aşırı dolu (overfilled) göl evreleri arasında geçtiğini göstermektedir. Çakrazboz ve alt İncigez kesitlerindeki karbonatça zengin istifler, yetersiz dolu evrelere özgü düşük enerjili profundal göl koşullarını temsil eder. Üst İncigez ve Başköy-1 kesitleri, üste doğru incelen transgresif istiflerin progradasyonlu litoral fasiyeslerle örtülmesiyle karakterize olan dengeli dolu koşulları yansıtır. Aşırı dolu koşullar, Bozköy ve Başköy-1'in üst seviyelerinde yer yer görülür ve bunlar, sürekli tatlı su girişiyle ilişkili yanal olarak genişleyen, üste doğru kalınlaşan ve tane boyu artan istiflerle tanımlanır. Dikey fasiyes geçişleri, istiflenme desenleri ve diyajenez izleri, yarı nemli ile yarı kurak iklim rejimleri altında yörüngesel zorlamalı göl seviyesi değişimlerini yansıtarak Geç Triyas kıtasal havza evrimi, fasiyes mimarisi ve iklim kontrollü sedimantasyon hakkında daha geniş bir anlayış sağlamaktadır.

Anahtar Kelimeler: *Batı Pontidler, Çakrazboz Formasyonu, fasiyes evrimi, göl tipi değişkenliği, paleoiklim, yörüngesel döngüler.*

INTRODUCTION

Terrestrial sedimentary successions of the Triassic period are rare in Türkiye. These successions, however, offer critical insights into the recovery of continental ecosystems following the end-Permian mass extinction, as well as into the evolution of interior basins under varying climatic and tectonic regimes. The Çakrazboz Formation, exposed in the Amasra–Kastamonu region of the Western Pontides, represents the only known Triassic nonmarine succession in Türkiye. This establishes it a key stratigraphic unit for reconstructing Late Triassic paleogeography, paleoclimate, and depositional dynamics within the Anatolian domain.

During the Mid–Late Triassic, the İstanbul–Zonguldak Terrane occupied a proximal position along the southern margin of Eurasia and experienced early rifting associated with the opening of the Neotethys Ocean (van Hinsbergen et al., 2020). The Western Pontides, located along the northern margin of the Neotethys, recorded the tectonic transition from Gondwanan to Laurasian paleolatitudes during the Late Triassic (Şengör, 1979; Scotese et al., 1979). As continental conditions prevailed across the region, sedimentation became predominantly nonmarine, culminating in the deposition of the Late Triassic Çakrazboz Formation – one of the most complete records of fluvio-lacustrine sedimentation within the Western Pontides.

Detrital zircon U–Pb and Lu–Hf isotopic analyses from Çakrazboz sandstones (Akdoğan et al., 2021) indicate derivation mainly from Carboniferous magmatic sources of the Sakarya Zone, suggesting that the İstanbul–Zonguldak Terrane had already amalgamated with an Armorican-type continental block prior to Late Triassic sedimentation. These results highlight the continuity between the magmatic and sedimentary evolution of the region and demonstrate that this terrane forms the easternmost segment of the Avalonian continental domain, accreted to Baltica during the late Neoproterozoic to early Cambrian interval (Yılmazer et al., 2025). Collectively, these findings provide a refined pre-Triassic basement framework for the subsequent development of the Western Pontides.

Palynological and sedimentological evidence indicates that deposition within the Çakrazboz

basin occurred during the Late Ladinian to Carnian, possibly extending into the earliest Norian (Şen, 2021), contemporaneous with widespread lacustrine sedimentation along the northern Neotethyan margin. Despite its significance, sedimentological data on the Çakrazboz Formation remain limited, and previous interpretations of its depositional environment are inconsistent. Biostratigraphic resolution is hindered by poor fossil preservation, and systematic sedimentological and petrographic analyses have not been undertaken. Consequently, key questions remain regarding the paleohydrology, climatic forcing, and tectonic influences that governed sedimentation in this intracontinental basin.

This study aims to address these gaps through integrated sedimentological and petrographic analyses across six measured stratigraphic sections of the Çakrazboz Formation. The primary objectives are to (1) document vertical and lateral lithofacies variations and reconstruct the spatial and temporal organization of depositional environments, and (2) establish a high-resolution facies architecture model elucidating interactions among fluvial channels, floodplains, ephemeral lakes, and palustrine wetlands. By directly linking lake-level fluctuations to climate oscillations, this research provides a concise yet original perspective on the cyclic nature of sedimentation in Triassic continental basins.

A key methodological advance of this work lies in the systematic and comparative analysis of six stratigraphic successions, integrating field-scale sedimentological data with petrographic characterization of 130 thin sections. This multi-site approach enables recognition of spatially variable facies patterns, diagenetic overprints, and climatically driven stacking motifs, offering a more comprehensive reconstruction of depositional dynamics than previously available for this formation.

To place these depositional patterns in their regional context, the geological and biostratigraphic framework of the Western Pontides is outlined below.

GEOLOGICAL SETTING and BIOSTRATIGRAPHY

The Pontides, a prominent orogenic belt in northern Türkiye, evolved through the closure and complex interactions of the Neotethys Ocean (Şengör, 1989; Robinson, 1997; Okay & Tüysüz, 1999; Simmons et al., 2018). As part of the Tethyan orogenic system, this belt comprises three east–west–trending tectonostratigraphic subdivisions – Western, Central, and Eastern Pontides (Yılmaz et al., 1997). The study area lies within the Western Pontides and is bounded to the south by the İzmir–Ankara–Erzincan suture zone and to the east by the Intra-Pontide suture (Figure 1). Regionally, the Western Pontides represent a foreland system composed of a Variscan metamorphic basement and Carboniferous–Permian plutonic units, overlain by Mesozoic shelf carbonates and, unconformably, by the Triassic continental strata of the Çakrazboz Formation (Figure 2) (Akman, 1992; Yılmaz et al., 1997; Okay and Tüysüz, 1999).

From a geodynamic perspective, the Western Pontides occupied the northern active margin of the Neotethys, which evolved through successive rifting, subduction, and accretion events during the Paleozoic–Mesozoic (Okay and Nikishin, 2015; Nikishin et al., 2015a, b). Early to Middle Triassic extension along the southern Eurasian margin led to intracontinental rifting and the development of fluvio-lacustrine basins. During the Late Triassic, these rift systems evolved into small-scale depressions bounded by normal faults, where continental red beds, marls, and lacustrine carbonates accumulated under fluctuating hydrological and climatic conditions (Nikishin et al., 2015a). The İstanbul–Zonguldak Terrane, which hosts the Çakrazboz Formation, represents an Avalonian-derived continental fragment amalgamated with Laurasia prior to Triassic sedimentation (Okay and Nikishin, 2015).

Figure 1. Major tectonic terranes in the Black Sea/Anatolia region (Okay and Tüysüz, 1999).
Şekil 1. *Karadeniz/Anadolu Bölgesi temel tektonik birimleri gösteren jeoloji haritası (Okay and Tüysüz, 1999).*

In a broader regional context, Nikishin et al. (2015b) emphasized that the Western Pontides formed part of a Late Triassic to Early Jurassic back-arc rift system that developed along the northern Neotethyan margin. This extensional phase predated the opening of the Western Black Sea Basin and strongly influenced the geometry and subsidence patterns of Triassic basins in the Amasra–Cide region.

Çakrazboz Formation

The Çakrazboz Formation was first defined by Varol and Akman (1988) during regional mapping of the Amasra–Çakraz area. Its type section was described by Akman (1992), who reported a maximum thickness of approximately 350 m and delineated its lithostratigraphic boundaries. Palynological and sedimentological data from Rutherford et al. (1992) and Alişan and Derman (1995) constrained its age to the Late Triassic and emphasized its distinct nonmarine character. Stolle (2016) later refined the stratigraphic framework by correlating the formation with equivalent fluvial units elsewhere in the Western Pontides using geochemical proxies.

The studied sections are situated in the Amasra and Kastamonu provinces of northwestern Anatolia, within the Western Pontides. These include the Çakraz, Bozköy, and İncigez sections near Amasra, and the Başköy-1, Başköy -2, and Başköy -3 sections near Cide in Kastamonu (Figure 3).

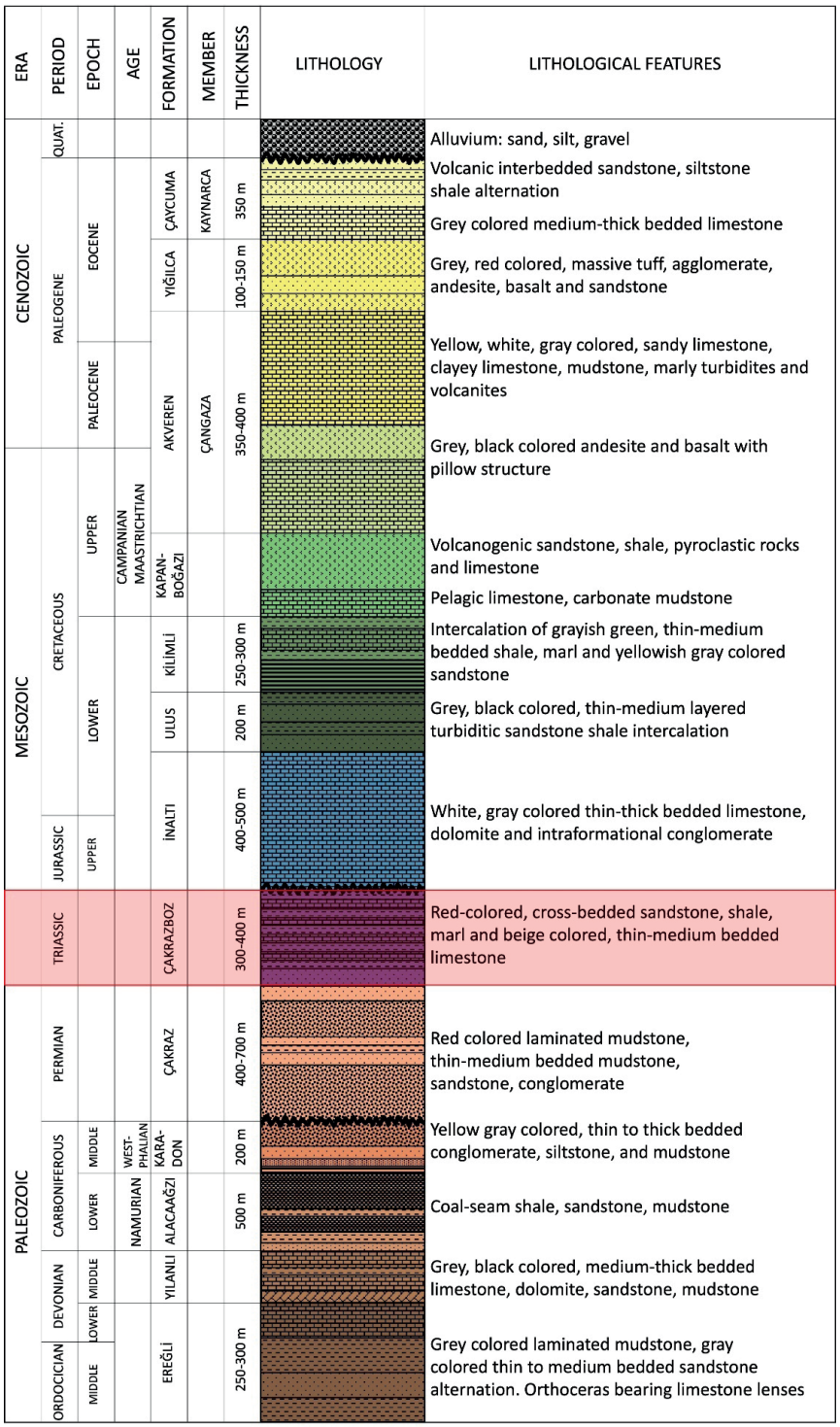

Figure 2. The studied sections are indicated by the red-shaded area on the generalized stratigraphic column of the Zonguldak–Amasra region (modified from Akbaş et al., 2002).

Şekil 2. *Çalışılan kesitler, Zonguldak-Amasra bölgesinin genelleştirilmiş stratigrafik kesiti üzerinde kırmızı renkli alan ile gösterilmiştir (Akbaş vd., 2002'ten yararlanılarak çizilmiştir).*

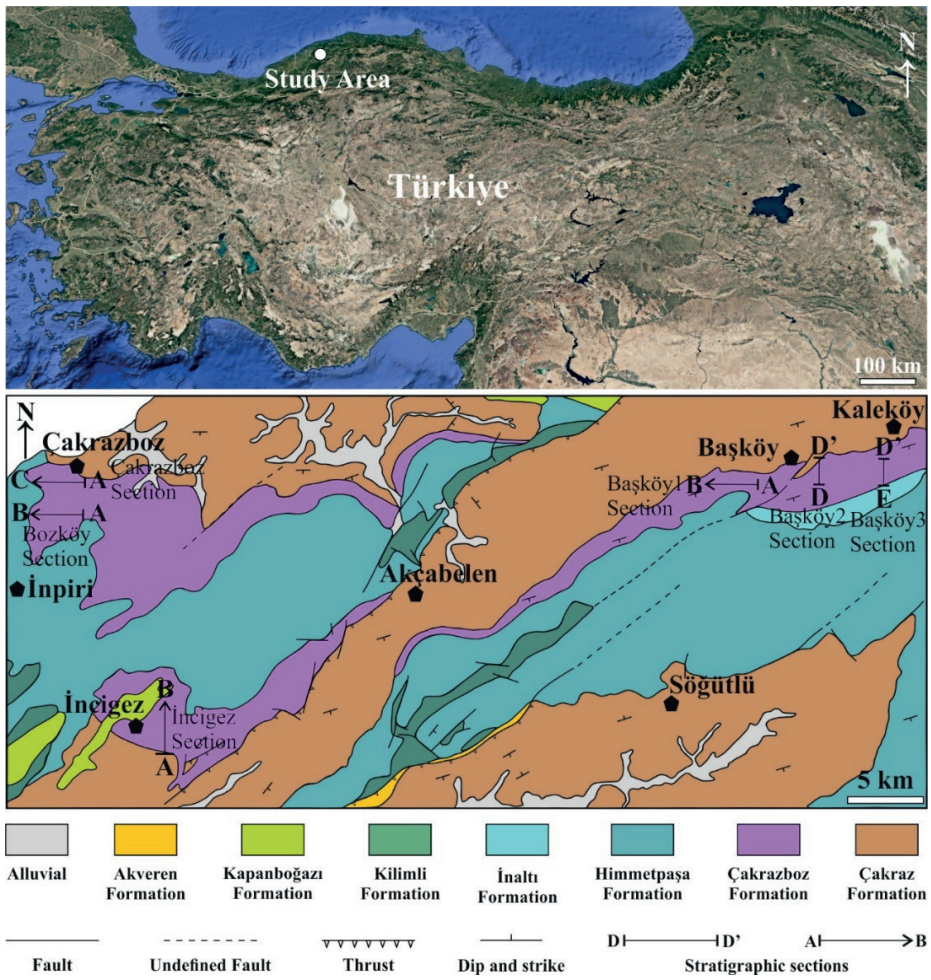

Figure 3. a) The study area indicated on the Türkiye location map prepared using Google Earth imagery, and **(b)** the geological map of the study area showing the locations where the stratigraphic sections were measured along with the strike directions of these sections.

Şekil 3. a) *Çalışma alanı, Google Earth görüntüsü kullanılarak hazırlanan Türkiye konum haritası üzerinde gösterilmiştir,* ***(b)*** *çalışma alanının jeoloji haritası ile stratigrafik kesitlerin ölçüldüğü lokasyonlar ve bu kesitlerin doğrultuları gösterilmiştir.*

On the Turkish geological map, Çakraz, Bozköy, and İncigez lie on the Zonguldak E28 1:100,000 sheet (Akbaş et al., 2002), whereas the Başköy sections are on the Zonguldak E29 sheet (Gedik and Aksay, 2002).

Locally, the formation exhibits thickness variations from 20 m at Başköy-3 to 66 m at Bozköy, controlled by synsedimentary faulting and differential subsidence within a rift-related lacustrine basin (Varol and Akman, 1988; Akman, 1992; Şen, 2021). Structural highs formed by folded and thrusted Paleozoic–Mesozoic units directed sediment routing into localized depocenters (Okay and Tüysüz, 1999). Paleogeographic reconstructions place the study area at ~20°–30° N paleolatitudes under a warm–humid to semi-arid climate (Scotese et al., 1979), consistent with alternating oxidized and reduced lacustrine deposits.

The Çakrazboz Formation thus records the nonmarine response to Early Triassic extensional tectonism, representing an intracontinental equivalent of syn-rift sedimentation prior to the onset of Cretaceous back-arc spreading (Okay and Nikishin, 2015; Nikishin et al., 2015a; Nikishin et al., 2015b).

Palynological and biostratigraphic data, although scarce, provide crucial constraints on the formation's age. Samples from the Çakrazboz Formation are generally barren (Alişan and Derman, 1995). However, palynofloral assemblages from the overlying Başköy Formation contain typical Late Triassic taxa such as *Ovalipollis*, *Triradispora*, *Infernopollenites*, and *Enzonalapollenites* (Alişan and Derman, 1995). Additional analyses by Şen (2021) revealed a palynofloral association characterized by *Ovalipollis ovalis*, *Triadispora*, and *Enzonalapollenites*, suggesting a Late Ladinian to Carnian, and possibly earliest Norian age. This interpretation aligns well with coeval palynostratigraphic records from Tethyan and European basins (Kürschner and Herngreen, 2010; Fijałkowska-Mader et al., 2015), reinforcing the regional correlation. Detrital zircon U–Pb ages obtained from sandstones of the formation further support this assignment, yielding dominant Carboniferous and Neoproterozoic–Cambrian age populations indicative of Sakarya-type continental sources and a Late Triassic depositional age (Akdoğan et al., 2021).

The underlying Çakraz Formation has recently been redefined as Permian in age based on macrofloral and ichnological evidence, including *Annularia*, *Stigmaria*, and the tetrapod footprints *Hyloidichnus* (Gand et al., 2011). These fossils indicate a Cisuralian (Early Permian) age for the lower red beds and suggest deposition in palustrine floodplain environments under warm and seasonally humid conditions. The Çakrazboz Formation, which conformably overlies these deposits, represents the transition to younger fluvio-lacustrine successions of Late Triassic age (Gand et al., 2011; Şen, 2021; Tüysüz, 2022).

MATERIALS and METHODS

Field Works and Sampling

Fieldwork was conducted in the Amasra (Bartın) and Cide (Kastamonu) districts within the Western Pontides of northwestern Anatolia. Six stratigraphic sections of the Çakrazboz Formation were measured bed-by-bed: Çakraz, Bozköy, İncigez, and Başköy-1, Başköy -2, and Başköy-3. A total of 342 rock samples were systematically collected along the measured sections (Table 1).

Table 1. Geographic coordinates, total number of samples, and stratigraphic thickness of the measured sections of the Çakrazboz Formation.

Çizelge 1. *Çakrazboz Formasyonu'nun ölçülü stratigrafik kesitlerinin kalınlığı, coğrafik koordinatları ve toplam numune sayıları*

Section No	Sampling Sites	Coordinates	Total Sample	Section Thickness (m)
1	Çakraz village	41°45'45.3"N 32°27'52.1"E	56	37
2	Bozköy village	41°46'00.7"N 32°27'36.2"E	52	66
3	İncigez village	41°42'40.8"N 32°28'53.4"E	112	60
4	Başköy village-1	41°46'15.6"N 32°42'18.0"E	48	33
5	Başköy village-2	41°45'49.5"N 32°42'21.1"E	35	59
6	Başköy village-3	41°45'49.5"N 32°42'21.1"E	36	20

At each section, sedimentological attributes such as lithology, grain size, sedimentary structures, bed thickness (±1 cm), and contact relationships were recorded in detail. Lithological colors were determined using the GSA Rock-Color Chart (2009), and all field sketches were digitized using CorelDRAW to produce standardized stratigraphic sections.

Chemical Analysis

Chemical fractionation was performed on rock samples to classify the studied sedimentary rocks according to their relative silica, carbonate, and organic matter contents. This approach allowed the determination of detrital, carbonate, and organic components forming the rocks. Elemental geochemical analyses were carried out to quantify organic carbon, inorganic carbon, and silica contents of the Çakrazboz Formation, following the procedures of Verardo et al. (1990), Hedges and Stern (1984), and Wang et al. (2012). Acidification was used to remove inorganic carbon and isolate organic fractions.

A total of 137 samples were analyzed (Çakraz: 28; Bozköy: 20; İncigez: 39; Başköy-1: 21; Başköy-2: 10; Başköy-3: 19). Approximately 10 g of each sample was crushed to <0.25 mm and oven-dried at 100 ºC to remove moisture. The samples were then treated with 10% dilute HCl to dissolve carbonate minerals ($CaCO_2$) and rinsed three times with deionized water. After drying, residues were exposed to 50% diluted H_2O_2 to oxidize organic matter until the solution became clear, following Wang et al. (2012).

The weight loss recorded after each treatment step was used to calculate carbonate and organic matter contents, while the insoluble residue was interpreted as primarily composed of clay and quartz. The resulting compositional data enabled differentiation of carbonate-rich, siliciclastic-rich, and organic-bearing sedimentary rocks and were further integrated with petrographic and facies observations to evaluate compositional variations across the formation.

Sedimentary Texture Analysis

Sedimentary texture and provenance analyses were performed to infer depositional processes, transport mechanisms, and source characteristics, following the procedures of Pettijohn et al. (1973), Reineck and Singh (1980), Boggs (2014), and Dickinson (1985). Sandstone texture was evaluated in terms of grain morphology, roundness, surface features, particle size, and overall detrital fabric. These parameters were used to interpret hydrodynamic conditions and depositional environments (Şen, 2021).

Grain morphology was quantified through projection measurements of sphericity and roundness. Sphericity was calculated as the ratio between the diameters of the inscribed and circumscribed circles of each grain (Sneed and Folk, 1958), whereas roundness was determined as the ratio between the curvature diameter of the sharpest corner and the inscribed circle diameter (Dobkins and Folk, 1970).

Grain-size parameters, including mean, sorting, skewness, and kurtosis, were computed using the graphical methods of Folk and Ward (1957). A total of 219 quartz grains from 11 sandstone samples (Başköy-2 and Başköy-3) were analyzed. Microscopic thin-section images were printed, and individual grains were outlined to measure diameters using a circle template and ruler. All measurements were statistically processed to obtain mean, median, mode, and sorting indices. Sphericity and roundness were also evaluated using visual comparison charts (Powers, 1953; Pettijohn et al., 1987, 2012). This combination of graphical and microscopic methods provided reliable interpretations of hydraulic energy fluctuations and depositional settings within the Triassic fluvio-lacustrine system.

For provenance analysis, point-counting was performed on the same thin sections following the Gazzi–Dickinson method (Dickinson, 1985) to determine the relative proportions of quartz (Q), feldspar (F), and lithic fragments (L). A total of 111 to 379 framework grains were counted per sample, depending on grain abundance and thin-section quality, to minimize statistical uncertainty. The obtained QFL percentages were plotted on the

ternary diagram of Dickinson (1985) to classify sandstone provenance.

Sedimentary Petrographic Analysis

Petrographic analyses were conducted to define and classify the studied rocks according to their mineralogical composition, cement type, textural features, and porosity characteristics.

This classification aimed to distinguish between compositional and textural variations among lacustrine, palustrine, and fluvial facies.

A total of 130 thin sections were examined under a Leica DM2700 polarizing microscope at ×4–×10 PPL magnification to characterize texture, mineral composition, fossil content (ostracods, charophytes), and diagenetic modifications, including sparry calcite cement, fenestral fabrics, root traces, and calcrete formation.

Facies classification followed the schemes of Folk (1959) and Dunham (1962) for carbonate textures; Miall (1996) and Boggs (2006) for siliciclastic facies; and Platt and Wright (1992), Stow (2005), Alonso-Zarza and Tanner (2009), and Flügel (2010) for microfacies analysis and diagenetic interpretation. Broader depositional models and facies transitions were assessed following Reading and Levell (1996), and Tucker and Wright (1990), emphasizing the genetic relationship between depositional processes and sedimentary architecture.

This This integrated petrographic approach enabled recognition of gradual transitions among fluvial, palustrine, and lacustrine facies associations, as well as the identification of shallowing-upward cycles characteristic of hydrologically balanced lacustrine systems. The methodology closely follows Şen (2021) for Triassic lacustrine successions of the Western Pontides, ensuring consistency between petrographic observations and facies interpretation.

RESULTS

Lithostratigraphy

The Çakrazboz Formation exhibits pronounced lateral and vertical facies variability across the Western Pontides, reflecting an environmental transition from deep-lacustrine carbonate deposition in the northwest (Çakrazboz–İncigez) to marginal lacustrine and fluvial systems towards the southeast (Başköy area). The overall stratigraphic architecture is characterized by repetitive shallowing-upward successions, recording alternating hydrological and climatic conditions during the Late Triassic.

Çakrazboz section

The Çakrazboz stratigraphic section represents a well-preserved lacustrine succession dominated by thick-bedded and dark-grey limestones (0.3–4.5 m thick), underlain by basal carbonate mudstones ranging in color from light greenish-grey to whitish (Figure 4). Light olive-grey and yellowish-grey mudstones exhibit well-developed lamination, whereas very light grey to white carbonate mudstones are massive. Laminated carbonate mudstones indicate deposition under low-energy and deeper lacustrine conditions, while massive varieties reflect suspension settling during quiescent phases. Dark grey limestones in the upper part mark shallower lacustrine intervals with intermittent oxygenation, and the repetitive shallowing-upward pattern records climatically induced lake-level fluctuations controlling carbonate productivity (Gierlowski-Kordesch, 2010) (Figure 5).

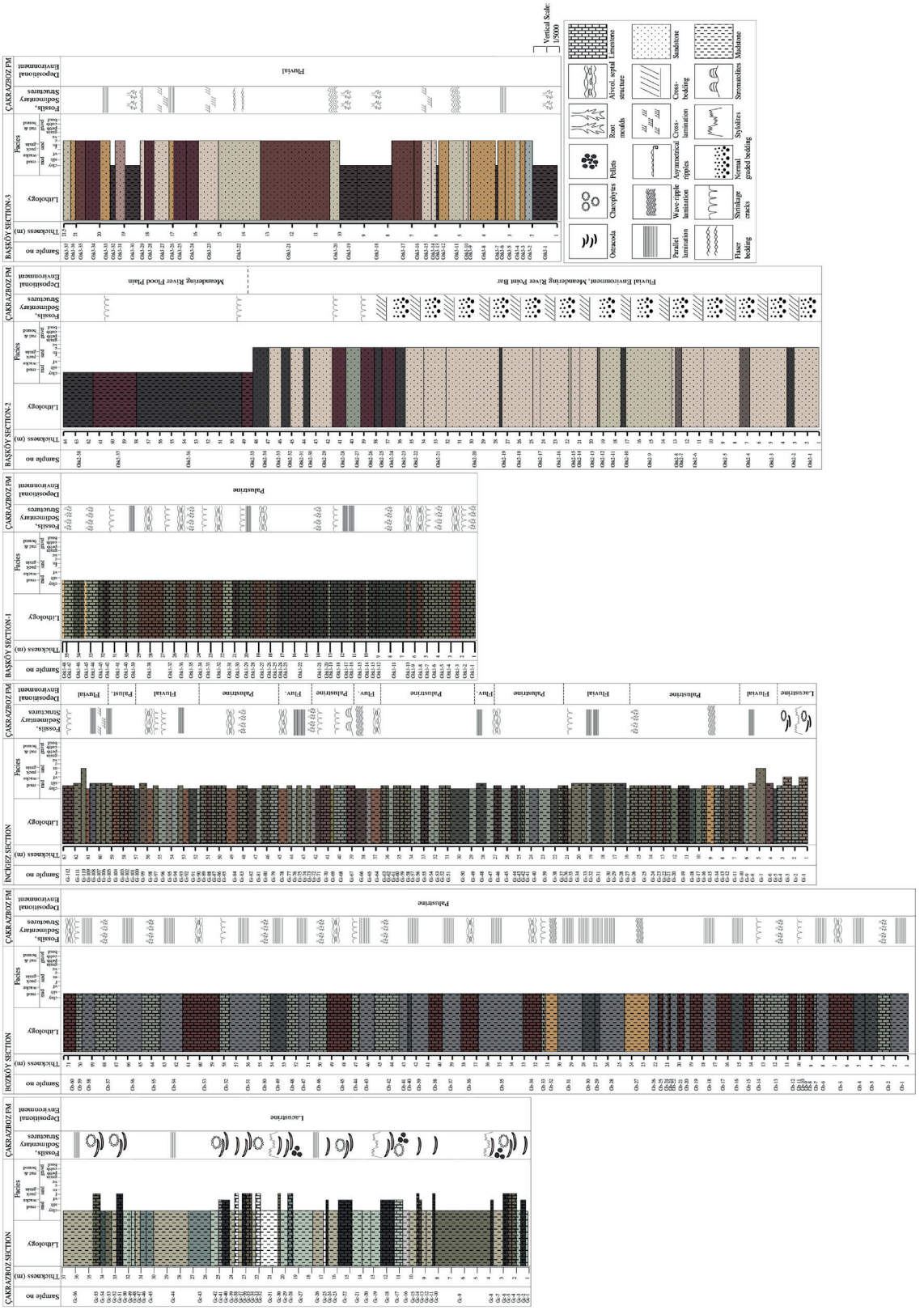

Figure 4. Measured stratigraphic sections of the Çakrazboz Formation.
Şekil 4. *Çakrazboz Formasyonuna ait ölçüli stratigrafik kesitler.*

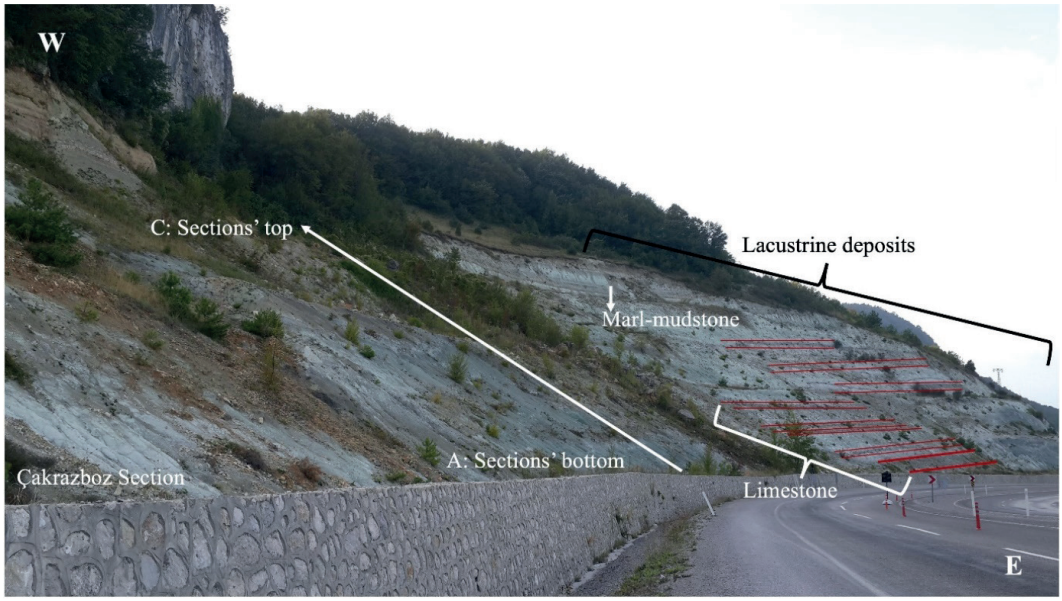

Figure 5. Field photograph of the Çakrazboz section showing lacustrine deposits characterized by limestone and mudstone alternations.

Şekil 5. *Kireçtaşı ve çamurtaşı ardalanmaları ile karakterize gölsel (lacustrine) çökelleri gösteren Çakrazboz kesitinin arazi fotoğrafı.*

The geochemical data are consistent with these sedimentological patterns. A clear inverse relationship between $CaCO_2$ and SiO_2 contents reflects alternating phases of chemical carbonate precipitation and siliciclastic influx. Based on these results, the rocks were classified as mudstone and marlstone with regard to Stow (2005) mudstone classification (Figure 6a), and as siliceous mudstone and carbonated mudstone following Gamero-Díaz et al. (2012) (Figure 6b). Mudstones contain 3–9 % organic matter (OM), and limestones 1–2 %. Elevated OM in fine-grained mudstones indicates deposition under dysoxic lacustrine conditions, whereas carbonate enrichment corresponds to drier intervals with enhanced evaporation and supersaturation. These lithological and geochemical features together represent a hydrologically balanced lacustrine system oscillating between humid and arid climatic phases.

Bozköy section

The Bozköy stratigraphic section displays a well-developed fluvio-palustrine succession composed of interbedded mudstone, marlstone, siltstone, and calcrete-like lithofacies (Figure 4). The basal part consists of grey laminated mudstones, overlain by alternating reddish-brown and greenish-grey marlstones that culminate in reddish-brown marl beds (Figure 7a and b). These marl–mudstone alternations dominate the section. The upper part includes more frequent siltstone/mudstone intervals (Figure 7c), representing fluvial siltstone facies, including a distinctive pale yellowish-orange laminated siltstone bed used for correlation with the Başköy-1 and İncigez sections (Figure 7d), along with carbonate mudstone/marl alternations. Lamination varies from parallel in grey mudstones to wavy in yellowish siltstones, whereas the marlstones exhibit desiccation cracks and root molds. These features indicate periodic subaerial exposure, pedogenic alteration, and shallow-water deposition under fluctuating groundwater

conditions. The alternation of reddish-brown and greenish-grey marl layers clearly reflects oxidation–reduction variations and short-term hydrological shifts along the lake margin.

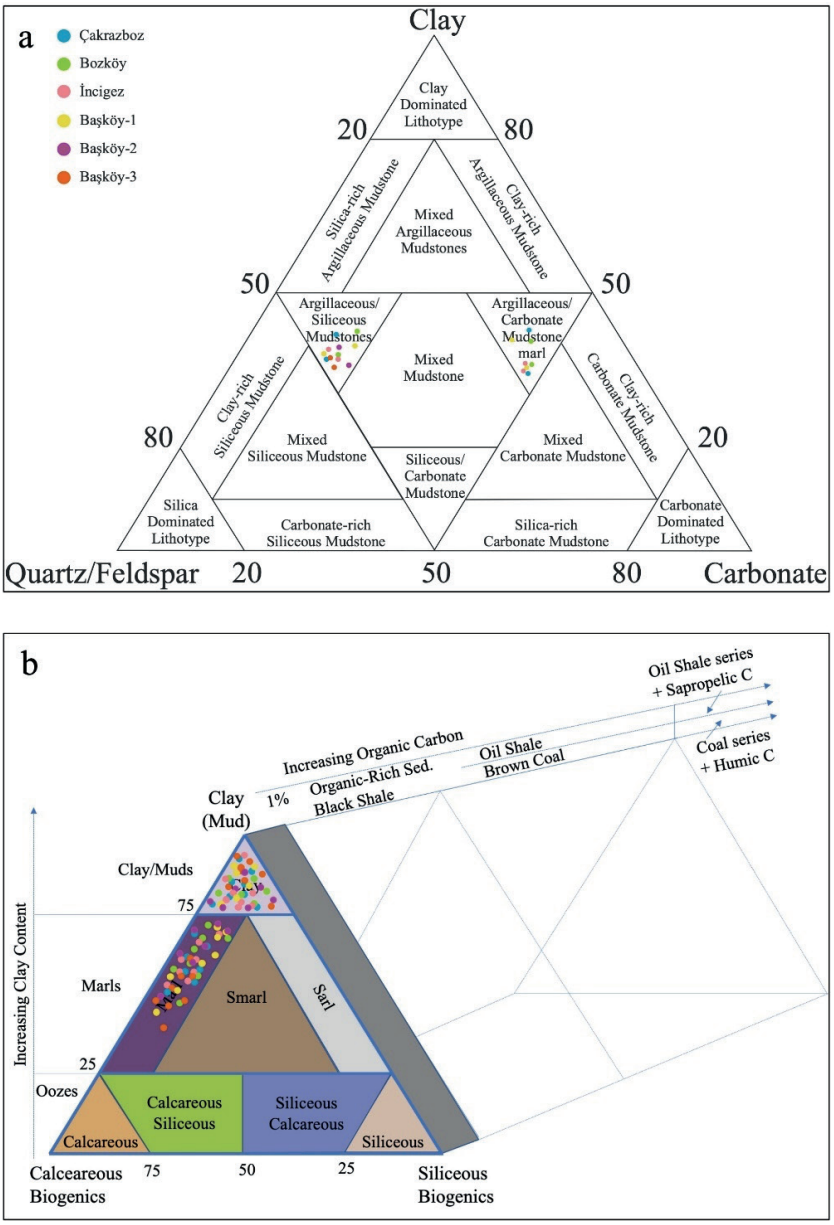

Figure 6. a) Stow (2005) compositional mudstone classification ternary diagram, based on biogenic carbonate and silica, and mud/clay components, showing the studied rocks classified as mudstone and marlstone; the representative symbols of the Çakrazboz Formation sections are shown, **(b)** Gamero-Díaz et al. (2012) ternary diagram illustrating the classification of the samples as siliceous mudstone and carbonated mudstone.

Şekil 6. a) *Biyojenik karbonat ve silis ile çamur/kil bileşenlerine dayalı Stow'un (2005) kompozisyonel çamurtaşı sınıflamasını gösteren üçgen diyagram, çalışılan kayaçların çamurtaşı ve marn olarak sınıflandırılması ve Çakrazboz Formasyonu kesitlerine ait temsilî sembollerin gösterimi,* ***(b)*** *Gamero-Díaz vd. (2012) üçgen diyagramında örneklerin silisli çamurtaşı ve karbonatlı çamurtaşı olarak sınıflandırılması gösterilmektedir.*

Figure 7. Field photographs of the Bozköy section, showing **(a)** the basal level consisting of grey laminated mudstone, **(b)** overlying alternating reddish-brown and greenish-grey marlstones that culminate in reddish-brown marl beds, **(c)** upper parts of the section characterized by more frequent siltstone/mudstone and carbonate mudstone–marl alternations, and **(d)** a fluvial pale yellowish-orange laminated siltstone bed used as a marker horizon for correlation with the Başköy-1 and İncigez sections.

***Şekil** 7. Bozköy istifine ait arazi fotoğraflarında; **(a)** taban kesiminde gri renkli laminalı çamurtaşı düzeyi, **(b)** bu düzeyin üstünde, ardalanan kırmızımsı-kahverengi ve yeşilimsi-gri marnlar ve bunların kırmızımsı-kahverengi marn seviyeleriyle sonlanması, **(c)** kesitin üst kesimlerinde daha sık görülen silttaşı/çamurtaşı ile karbonatlı çamurtaşı–marn ardalanmaları, ve **(d)** Başköy-1 ve İncigez kesitleriyle korelasyon için kılavuz düzey olarak kullanılan flüvyal kökenli soluk sarımsı-turuncu renkli laminalı silttaşı seviyesi gösterilmiştir.*

Based on their chemical composition, the rocks were classified using the mudstone scheme of Stow (2005) (Figure 6a) and the mudstone classification of Gamero-Díaz et al. (2012) (Figure 6b). Accordingly, the rocks were defined as mudstone and marlstone following Stow (2005), and as siliceous mudstone and carbonated mudstone following Gamero-Díaz et al. (2012). Mudstones contained 1–3 % organic matter (OM) and marlstones 1–4 %, showing moderate preservation of organic matter under variable redox conditions. Carbonate enrichment in the upper layers corresponds to pedogenic modification, and alternating carbonate–siliciclastic inputs reflect lake-margin variability controlled by climatic oscillations. Collectively, the sedimentological and geochemical data reveal periodic wet–dry alternations in a palustrine environment progressively transitioning toward marginal lacustrine conditions.

İncigez section

The İncigez stratigraphic section (Figure 4) exhibits a vertically organized succession of lacustrine, palustrine, and fluvial deposits (Figure 8a). The lower part consists of carbonate mudstones and limestones, representing shallow lacustrine environments (Figure 8b). The middle intervals are dominated by palustrine facies such as laminar calcretes, green–brown marlstones, and paleosols containing root traces – typical of fluctuating water tables. The upper part comprises siltstone, mudstone, and silcrete-like beds that display cross- and parallel laminations as well as desiccation cracks, indicating episodic subaerial exposure and intermittent fluvial influx. (Figure 8c). This vertical pattern records a progressive infilling of a lacustrine basin evolving into marshy and fluvial environments under climate-driven hydrological fluctuations.

The rocks were classified as mudstone and marlstone according to Stow (2005) mudstone classification (Figure 6a), and as siliceous mudstone and carbonated mudstone based on Gamero-Díaz et al. (2012) (Figure 6b). Mudstones contain 1–2 % organic matter (OM) and sandstones/siltstones 1–3 %, with an upward increase in detrital input and decreasing carbonate content, marking a transition from lacustrine to palustrine–fluvial conditions. These relationships confirm that the İncigez succession records alternating humid and arid phases linked to orbitally modulated climatic forcing.

Başköy-1 section

The Başköy-1 stratigraphic section (Figure 4) represents a marginal lacustrine succession characterized by paleosol-bearing limestones and calcretes at the base, overlain by thin-bedded marlstones, mudstones, and siltstones (Figures 9a). The basal interval includes limestone and mudstones indicative of lacustrine conditions. The middle part comprises palustrine marlstones interbedded with laminated and massive siltstones, whereas the uppermost part transitions into fluvial siltstone facies, including a distinctive pale yellowish-orange laminated siltstone beds – used for correlation with the İncigez and Bozköy sections (Figure 7d). Desiccation cracks are common in greenish-grey and reddish-brown marl–paleosol beds (Figure 9b), while the diverse coloration results from Fe–Mn oxidation under fluctuating vadose–phreatic conditions.

The rocks were classified as mudstone and marlstone according to Stow (2005) mudstone classification (Figure 6a), and as siliceous mudstone and carbonated mudstone based on Gamero-Díaz et al. (2012) (Figure 6b). Organic matter ranges from 1–3 %, being higher in marlstones than in mudstones. Carbonate-rich layers coincide with reduced detrital influx and correspond to shallowing-upward cycles. The integration of lithological and geochemical patterns indicates alternating wet–dry climatic cycles that governed carbonate precipitation and pedogenesis at the lake margin during progressive basin infilling.

Başköy-2 section

The Başköy-2 stratigraphic section is dominated by fluvial sandstone–mudstone alternations (Figures 4). Sandstone beds are medium to thick, cross-bedded, and normal graded, passing upward into pedogenically altered mudstones. These successions exhibit clear fining- and thinning-upward trends, recording channel abandonment, lateral accretion, and overbank deposition during waning-energy stages (Figure 10). Sandstones occur as tabular cross-bedded sets with planar lamination and erosional bases, characteristic of point-bar architectures developed through lateral channel migration. Alternating sandstone–mudstone couplets record episodic flooding and overbank sedimentation under variable discharge regimes.

Figure 8. Field photographs of the İncigez section, showing **(a)** a succession of lacustrine, palustrine, and fluvial deposits, **(b)** the lower part composed of carbonate mudstones and limestones representing shallow lacustrine environments, and **(c)** the upper part characterized by siltstone, mudstone beds belonging to palustrine and fluvial environments.

Şekil 8. *İncigez stratigrafik kesitine ait arazi fotoğrafları;* ***(a)*** *lakustrin, palustrin ve flüviyal çökel istifi,* ***(b)*** *sığ gölsel ortamları temsil eden karbonatlı çamurtaşı ve kireçtaşlarından oluşan alt kesim, ve* ***(c)*** *palustrin ve flüviyal ortamlara ait silttaşı, çamurtaşı tabakalarının yer aldığı üst kesim gösterilmiştir.*

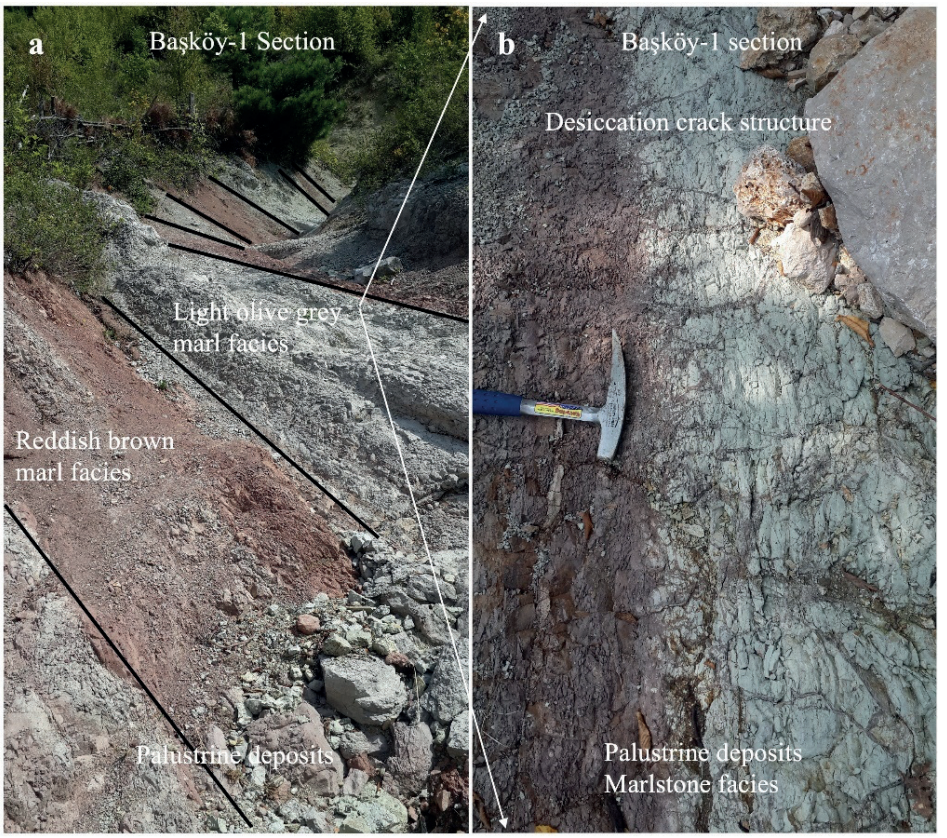

Figure 9. Field photographs from the Başköy-1 section showing **(a)** basal paleosol-bearing limestones and calcretes overlain by marlstone and mudstone units, and **(b)** close-up of desiccation cracks developed in greenish-grey marlstone layer in a palustrine setting.

Şekil 9. *Başköy-1 kesitinden arazi fotoğraflarında;* ***(a)*** *taban kesimde yer alan paleosol içeren kireçtaşları ve kalkerlerin üzerinde gelişen yeşilimsi gri ve kırmızımsı kahverengi marn ardalanması,* ***(b)*** *palüstrin ortamda yeşilimsi gri marn tabakasında gelişmiş kuruma çatlaklarının yakın plan görünümünü göstermektedir.*

The mudstone lithofacies were determined as clay based on Stow (2005) classification (Figure 6a) and as argillaceous/siliceous mudstone according to Gamero-Díaz et al. (2012) (Figure 6b). Geochemically, quartz arenites contain 1–3 % organic matter (OM) and mudstones 1–4 %, with carbonate precipitation restricted to pedogenic calcretes formed during subaerial exposure. The inverse $CaCO_2$–SiO_2 relationship reflects alternating siliciclastic influx and carbonate stability during dry intervals. Such rhythmic alternations indicate climate-controlled discharge variations in a meandering fluvial network influenced by seasonal aridity.

Grain-texture analyses from eight thin-section samples (Figure 11) reveal subangular to subrounded grains with low to moderate sphericity (0.25–0.70) and generally poor sorting (Table 2). Most samples are immature to submature, though a few exhibit moderately well-sorted textures. Sample GBK2-2 contains the most rounded grains (0.60–1.00), whereas GBK2-28 shows the lowest sphericity (<0.30). Statistical parameters indicate coarse-skewed and leptokurtic to platykurtic distributions, suggesting variable hydraulic sorting and fluctuating flow energy.

Figure 10. Field photograph from the Başköy-2 section showing fluvial sandstone–mudstone alternations. Medium- to thick-bedded, cross-bedded, normally graded sandstones pass upward into pedogenically modified mudstones, forming fining- and thinning-upward successions indicative of channel abandonment, lateral accretion, and overbank deposition.

Şekil 10. *Başköy-2 kesitinden flüvyal kumtaşı–çamurtaşı ardalanmasını gösteren arazi fotoğrafı. Orta–kalın tabakalı, çapraz katmanlı ve normal derecelenmiş kumtaşları yukarı doğru pedojeneze uğramış çamurtaşlarına geçerek kanal terkini, yanal birikimi ve taşkın düzlüğü çökellerini yansıtan, incelen tane boyu ve kısalan tabaka kalınlığıyla, yukarı doğru sığlaşan bir istifi işaret etmektedir.*

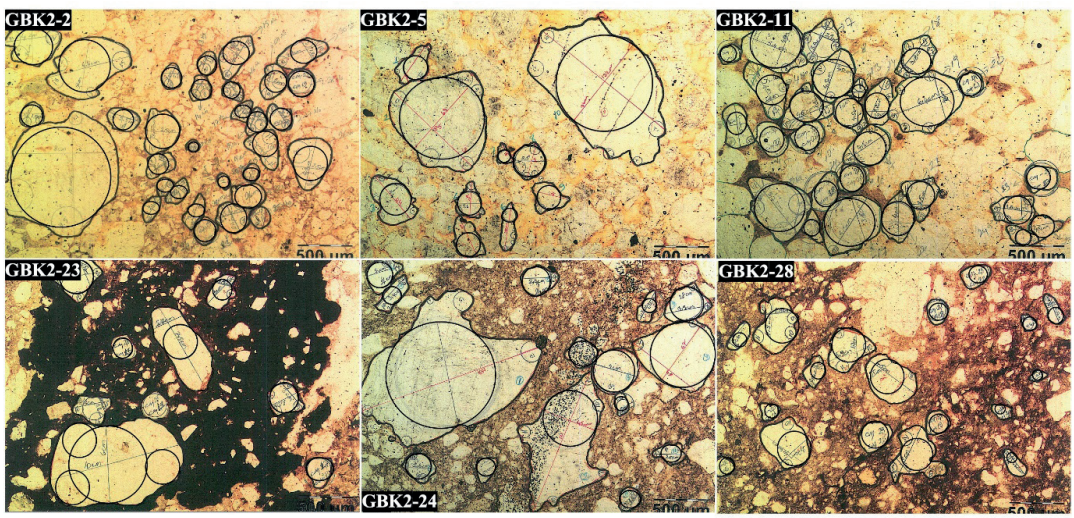

Figure 11. The illustration shows drawings related to the grain-texture analysis performed on thin-section microphotographs.

Şekil 11. *Şekil, ince kesit mikrofotoğrafları üzerinde yapılan tane-doku analizine ilişkin çizimleri göstermektedir.*

These textural features are consistent with quartz arenite–quartz wacke alternations and indicate short-distance transport within a low-gradient fluvial system. According to Pettijohn's (1987) classification, these sandstones correspond to quartz arenite and quartz wacke types, reflecting variable textural maturity and compositional purity (Figure 12).

Başköy-3 section

The Başköy-3 stratigraphic section consists of fluvial siliciclastic deposits composed of sandstone, sandy mudstone, and reddish to blackish-red mudstone lithofacies (Figures 4). These facies occur cyclically and display distinct coloration – pinkish-grey, yellowish-grey, dark yellowish-orange, and blackish-red – caused by oxidation–reduction variations during deposition. Hematite and limonite impart reddish–orange hues, indicating oxidizing floodplain conditions with local Eh–pH fluctuations (Franke and Paul, 1980; Rech-Frollo, 1971). Sandstone layers are medium- to thick-bedded, while sandy mudstone and mudstone layers are thinner and often display root traces, pedogenic mottling, and desiccation structures (Figure 13a). Cross-lamination, wavy lamination, and asymmetrical ripple marks are common in sandstone facies, suggesting dynamic but periodically emergent floodplain environments (Figure 13b).

Sedimentary-rock classification for the Başköy-3 section was conducted using the compositional mudstone scheme of Stow (2005) (Figure 6a), the mudstone classification of Gamero-Díaz et al. (2012) (Figure 6b), and the sandstone ternary classification diagram of Pettijohn et al. (1987) (Figure 12). According to these schemes, the mudstone lithofacies were classified as clay-rich mudstones in the sense of Stow (2005) and as argillaceous to siliceous mudstones following Gamero-Díaz et al. (2012), whereas the sandstone lithofacies were identified as quartz arenites and wackes based on the classification of Pettijohn et al. (1987).

Quartz arenites contain 1–10 % organic matter (OM), wackes 2–9 %, and mudstones 1–6 %. Carbonate is minimal in sandstones but occurs in fine-grained beds as pedogenic or diagenetic calcite. The alternation of red and green oxidation layers and pedogenic calcrete beds reflects periodic water-table fluctuations under semi-arid climatic conditions. Combined lithological, textural, and geochemical evidence demonstrates that Başköy-3 records repetitive floodplain deposition and subaerial exposure events governed by climate-controlled hydrological oscillations in a semi-arid continental basin.

Table 2. Sedimentary texture parameters of sandstones in the Başköy-2 and Başköy-3 sections.

Çizelge 2. *Başköy-2 ve Başköy-3 istiflerindeki kumtaşılarının sedimanter doku parametreleri.*

	Grain Size Parameters					
Sample No	**Si**	**Ski**	**K_G**	**Mz**	**Md**	**C**
GBK2-1	0.56	-0.26	0.93	1.17	1.26	0.86
GBK2-2	0.88	-0.19	1.13	1.31	1.48	1.75
GBK2-5	0.79	-0.22	0.65	1.02	1.22	1.53
GBK2-11	0.58	0.12	0.77	0.86	0.82	0.80
GBK2-23	0.61	-0.22	1.31	1.37	1.42	1.25
GBK2-24	0.50	-0.33	1.42	1.35	1.40	1.51
GBK2-28	0.70	-0.06	1.12	1.41	1.44	0.63
GBK2-31	0.49	0.23	0.94	0.68	0.62	0.73
GBK3-9	0.58	0.03	0.74	0.94	0.93	0.78
GBK3-11	0.55	-0.24	1.00	1.26	1.34	0.70
GBK3-20	0.27	0.00	0.84	1.50	1.50	0.46

Si: Sorting, Ski: Skewness, K_G: Kurtosis, Mz: Mean grain size, Md: Median grain size, C: Coefficient of gradation

Grain-texture analyses of three thin sections (Figure 14) reveal subrounded to rounded grains with low to moderate sphericity (0.25–0.70). GBK3-9 is poorly sorted and texturally submature, GBK3-11 is moderately sorted with slightly higher grain sphericity, and GBK3-20 is very well

sorted, exhibiting nearly symmetric grain-size distributions. Statistical data show coarse-skewed to symmetric, leptokurtic to platykurtic curves, reflecting reworking under fluctuating flow energy.

To interpret the depositional setting, sediment transport dynamics, and source characteristics of the Başköy-2 and Başköy-3 sections, grain-size and petrographic data were jointly evaluated. Grain-size parameters obtained from sedimentary texture analyses were plotted on the classification diagrams of Folk and Ward (1957) (Figure 15a), Stewart (1958) (Figure 15b), and Passega (1964) (Figure 15c). The results consistently indicate that the sandstones were deposited under fluvial conditions. According to the Folk and Ward (1957), and Stewart (1958) diagrams, the sandstones were formed through fluvial processes, whereas the Passega (1964) diagram reveals transportation as both bedload and suspension load. These interpretations, supported by poor to moderate sorting, subangular to subrounded grain shapes, and variable sphericity values (0.25–0.70), point to short-distance sediment transport within a low-gradient, meandering fluvial system influenced by fluctuating hydraulic energy and seasonal climatic oscillations.

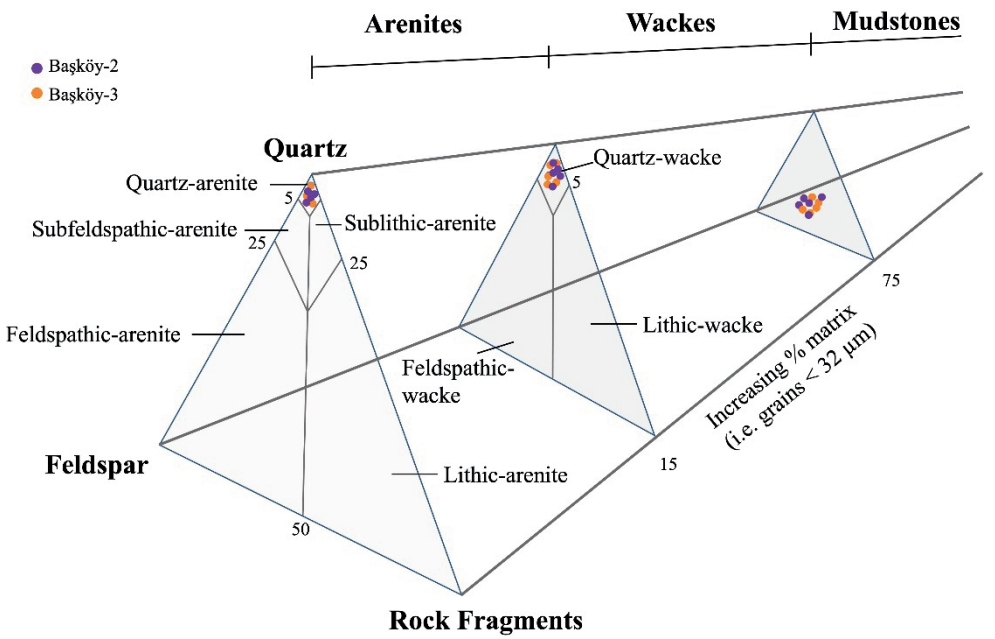

Figure 12. Pettijohn's (1987) ternary sandstone classification diagram, constructed using the relative proportions of grain size, composition, and matrix content. The representative symbols of the Başköy-2 and Başköy-3 samples are indicated.

Şekil 12. *Pettijohn'un (1987) üçgen kumtaşı sınıflama diyagramı, tane boyu, bileşim ve matriks içeriğinin göreceli oranlarına göre oluşturulmuştur. Başköy-2 ve Başköy-3 örneklerine ait semboller diyagram üzerinde gösterilmiştir.*

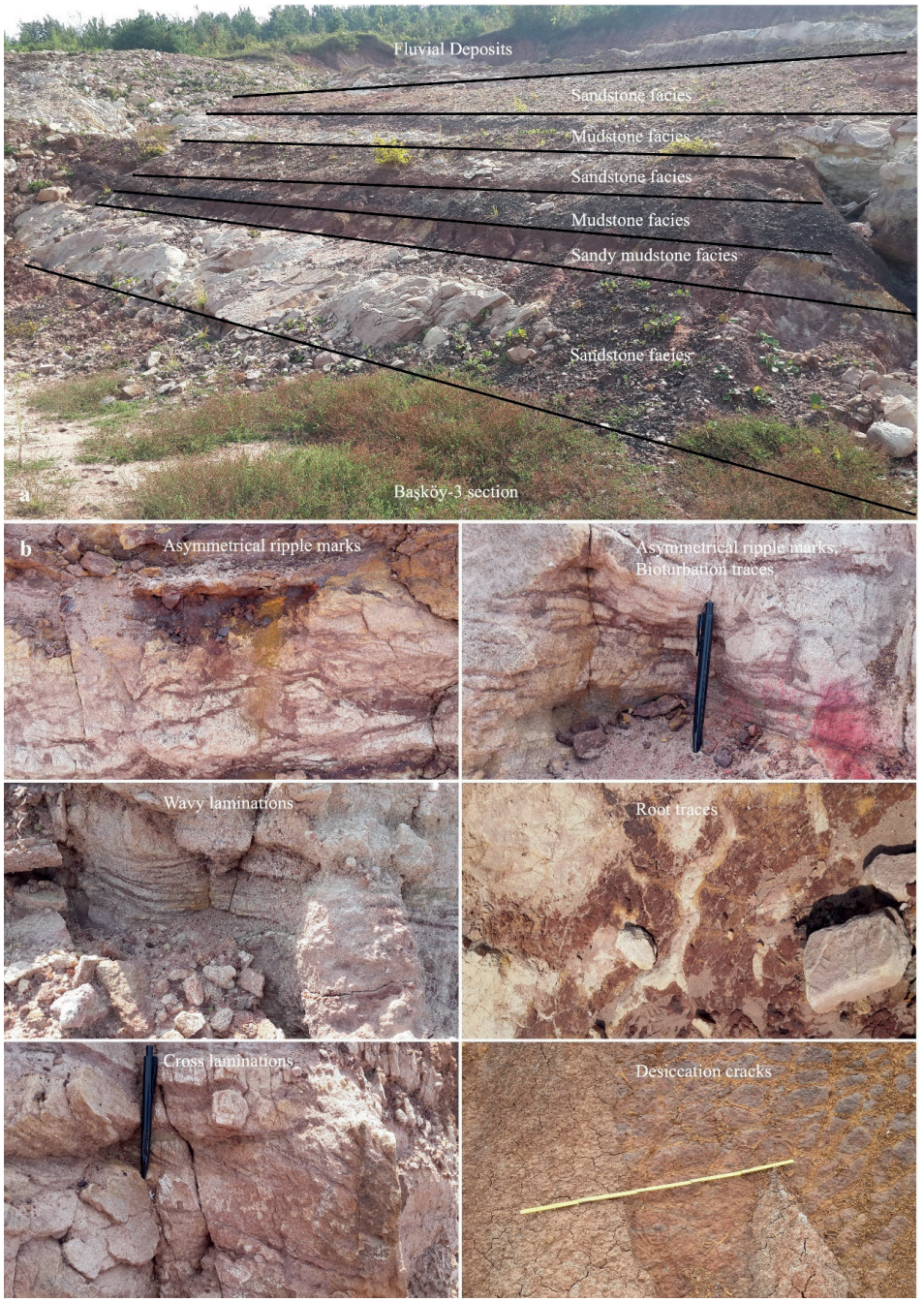

Figure 13. Field photographs from the Başköy-3 section showing fluvial sandstone–mudstone alternations: **a)** sandstone beds are medium- to thick-bedded, whereas sandy mudstone and mudstone layers are thinner, **(b)** asymmetrical ripple marks, bioturbation traces, wavy lamination, cross-lamination, root traces, and desiccation structures are observed, indicating dynamic but periodically emergent floodplain environments.

Şekil 13. *Başköy-3 kesitinden flüvyal kumtaşı–çamurtaşı ardalanmasını gösteren arazi fotoğrafları:* ***a)*** *kumtaşı tabakaları orta–kalın tabakalı olup, kumlu çamurtaşı ve çamurtaşı seviyeleri daha incedir,* ***(b)*** *asimetrik ripple izleri, biyotürbasyon izleri, dalgalı laminasyon, çapraz laminasyon, kök izleri ve kuruma çatlakları gözlenmekte olup, bu özellikler dinamik fakat periyodik olarak yüzeylenen taşkın düzlüğü ortamlarını işaret etmektedir.*

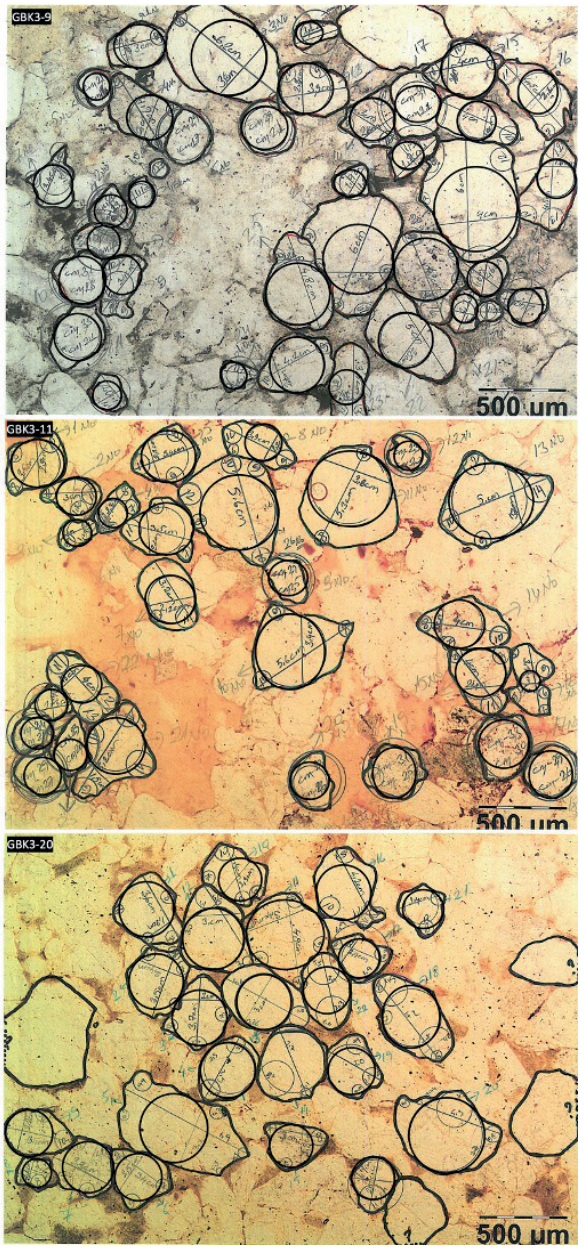

Figure 14. The illustration shows drawings related to the grain-texture analysis performed on thin-section microphotographs.

Şekil 14. *Şekil, ince kesit mikrofotoğrafları üzerinde yapılan tane-doku analizine ilişkin çizimleri göstermektedir.*

Complementarily, point-counting analyses were performed to determine sandstone provenance using Dickinson's (1985) QFL ternary classification (Table 3). The proportions of quartz, feldspar, and lithic fragments plotted on the QFL diagram show that the sandstones from the Başköy-2 and Başköy-3 sections fall within the "craton-interior" field, suggesting derivation from a stable continental source area consistent with the overall fluvial depositional system (Figure 15d).

Sedimentary Petrography

Petrographic analysis of the Çakrazboz Formation was conducted to characterize the mineral composition, microfacies types, and diagenetic features across its lacustrine–fluvial succession. The petrographic observations reveal a progressive transition from carbonate-dominated lacustrine facies in the Çakrazboz and İncigez sections to siliciclastic-rich fluvial facies in the Başköy sections, reflecting basinward evolution from deep to marginal depositional environments.

Çakrazboz section

The Çakrazboz stratigraphic section exhibits a well-preserved lacustrine carbonate succession composed mainly of micrite (carbonate mudstone), wackestone (biomicrite), and packstone (sparse biomicrite) microfacies.

- Carbonate mudstone facies consist of a micritic matrix with less than 10% bioclastic components, including rare ostracod shells and fine-grained quartz (Figure 16a). These facies indicate deposition in a low-energy and relatively deep lacustrine environment, where stratified water columns and potential anoxia contributed to the preservation of primary lamination.

- Wackestone facies contain more than 10% allochems – primarily ostracods, charophytes, intraclasts, and pellets – embedded in a micritic matrix (Figure 16b). The presence of these biogenic components suggests moderate-energy sublittoral conditions within a shallow freshwater lake.
- Packstone facies are rich in ostracods, charophytes, and pellets, with allochem contents exceeding 50%, indicating enhanced biogenic productivity and intermittent reworking in a shallower and well-oxygenated lacustrine setting (Figure 16c).

The micritic-to-sparitic transitions reflect subtle fluctuations in energy and water depth. Vertically, the succession displays a systematic shallowing-upward trend, from deep-water carbonate mudstones at the base to bioclastic packstones at the top. This stacking pattern recurs throughout the Çakrazboz section, implying repetitive depositional cycles driven by hydrological and climatic variability in a balanced-fill lacustrine system.

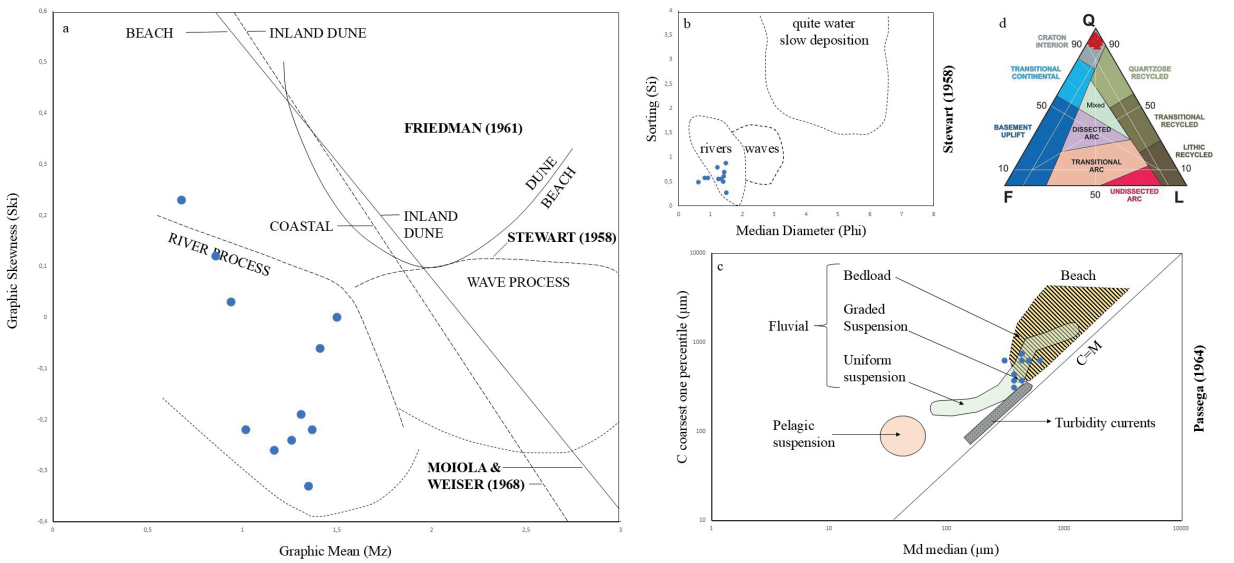

Figure 15. a–d) Grain-size and compositional diagrams showing the distribution of the studied samples on standard models; **(a)** mean–skewness, **(b)** sorting–median, **(c)** CM diagram, and **(d)** QFL ternary plot (references as cited).

Şekil 15. a–d) *İncelenen örneklerin standart modellere göre dağılımını gösteren tane boyu ve bileşimi diyagramları;* ***(a)*** *ortalama–çarpıklık,* ***(b)*** *boylanma–medyan,* ***(c)*** *CM diyagramı, ve* ***(d)*** *QFL üçgen diyagramı (ilgili atıf yapılan kaynaklara göre).*

Table 3. Results of point counting analysis of the sandstones in the Başköy-2 and Başköy-3 sections.
Çizelge 3. *Başköy-2 ve Başköy-3 istiflerindeki kumtaşlarının nokta sayım analiz Sonuçları.*

Sample No	Quartz	Feldspar	Lithic Fragment	VQ	MQ	DQ	CH	Total	Q%	F%	LF%
GBK2-1	348	2	5	330	-	13	5	355	98.03	0.56	1.41
GBK2-2	289	2	10	259	14	6	10	301	96.01	0.66	3.32
GBK2-5	339	6	8	332	-	7	-	353	96.03	1.70	2.27
GBK2-11	364	3	4	364	-	-	-	371	98.11	0.81	1.08
GBK2-23	108	1	2	108	-	-	-	111	97.30	0.90	1.80
GBK2-24	268	5	6	268	-	-	-	279	96.96	1.79	2.15
GBK2-28	169	2	1	169	-	-	-	172	98.26	1.16	0.58
GBK2-31	265	4	7	228	37	-	-	276	96.01	1.45	2.54
GBK3-9	348	1	10	314	34	-	-	359	96.94	0.28	2.79
GBK3-11	321	1	3	305	13	-	3	325	98.77	0.31	0.92
GBK3-20	376	1	2	376	-	-	-	379	99.21	0.26	0.53

VQ: Volcanic quartz, MQ:Metamorphic quartz, PQ: Detrital polycrystalline quartz, CH: Chert, Q: Quartz, F: Feldspar, LF: Lithic fragment

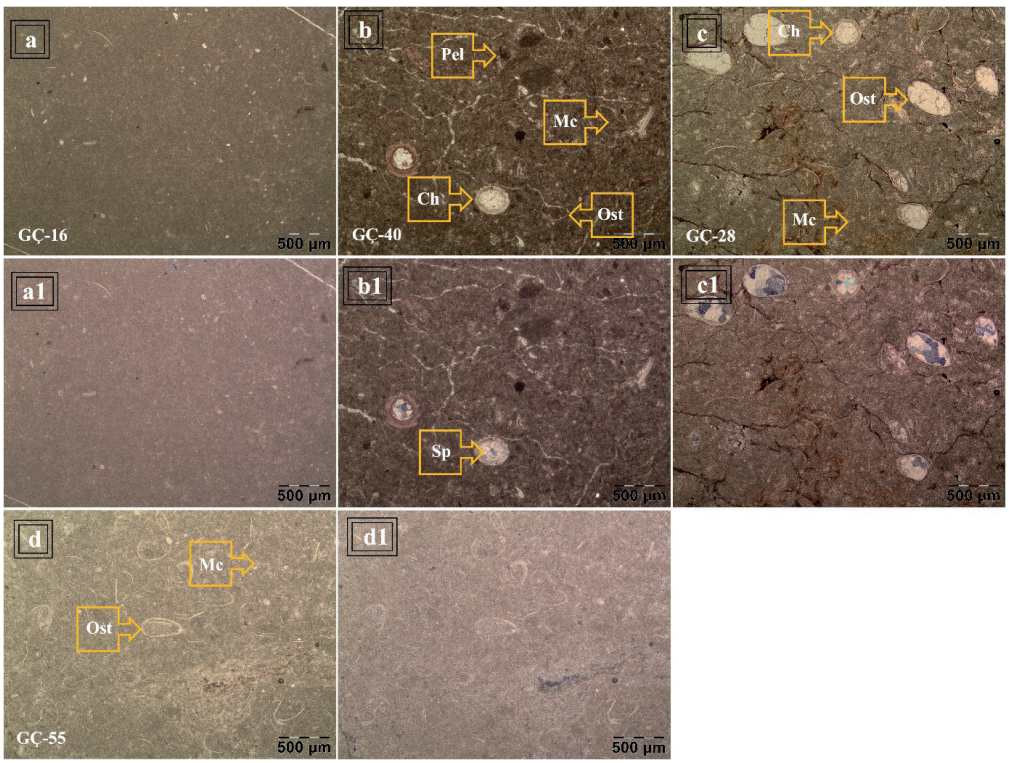

Figure 16. Photomicrographs of thin sections; **a)** carbonated mudstone (micrite) lithofacies (GÇ-16, PPl ×4), **(b)** wackestone microfacies (GÇ-40, PPl ×4), **(c)** packstone microfacies (GÇ-28, PPl ×10), and **(d)** packstone microfacies (GÇ-55, PPl ×4). Abbreviations: ostracods (Ost), charophytes (Ch), pellets (Pel), quartz (Q), sparite (Sp), matrix (Mc).

Şekil 16. *İnce kesitlere ait mikrofotoğraflar;* ***a)*** *karbonatlı çamurtaşı (mikrit) litofasiyesi (GÇ-16, PPl ×4),* ***(b)*** *vaketaşı mikrofasiyesi (GÇ-40, PPl ×4),* ***(c)*** *tanetaşı mikrofasiyesi (GÇ-28, PPl ×10), ve* ***(d)*** *tanetaşı mikrofasiyesi (GÇ-55, PPl ×4). Kısaltmalar: ostrakodlar (Ost), karofitler (Ch), pelletler (Pel), kuvars (Q), sparit (Sp), matriks (Mc).*

İncigez section

The İncigez stratigraphic section displays a vertical transition from carbonate-rich lacustrine facies at the base to palustrine and fluvial siliciclastic deposits upward, reflecting progressive basin infilling under fluctuating climatic and hydrological conditions.

- Mottled limestone exhibits desiccation cracks and Fe-mottling, reflecting intermittent subaerial exposure and pedogenic alteration (Freytet, 1973) (Figure 17a).
- Limestone with vertical root cavities and root molds records colonization by vegetation during emergent phases (Figure 17b).
- Laminar calcrete developed under prolonged exposure and vadose conditions, signifying pedogenic carbonate accumulation (Figure 17c).
- Green to brown marlstone represents alternating oxidation–reduction states along fluctuating water tables (Figure 17d).
- Nodular and brecciated limestone indicates repeated wetting–drying cycles and early diagenetic fragmentation in a palustrine setting.
- Micrite facies consist of microcrystalline carbonate cement with rare bioclasts, indicating quiet-water deposition in a low-energy lacustrine environment.
- Wackestone microfacies contain ostracods, charophytes, peloids, and intraclasts, representing deposition in a shallow and well-stratified lake (Figure 17e).
- Mudstone with Fe-staining and polygonal desiccation cracks records subaerial exposure on floodplains during dry phases.
- Silcrete-like beds display mud illuviations and pedogenic silicification, formed under alternating wet–dry regimes (Figure 17f).
- Laminated siltstones exhibit parallel lamination, indicating low-energy fluvial sedimentation (Figure 17g). Localized cross-lamination within the siltstones suggests short-lived increases in current velocity during fluvial deposition (Figure 17h).

The vertical facies succession defines a systematic upward transition:

- Lacustrine facies dominate the lower part,
- Palustrine facies are intercalated in the middle,
- and fluvial facies prevail in the upper part.

This organization reflects the progressive infilling and terrestrialization of a shallow lacustrine basin, marking the environmental shift from subaqueous to subaerial conditions under seasonally variable climates.

Başköy-1 section

The Başköy-1 stratigraphic section displays a transition from carbonate-rich paleosols and calcretes at the base, through palustrine carbonates, to overlying fluvial siliciclastic facies. The basal interval begins with limestone containing vertical root cavities, followed by alternating mottled limestone, brecciated limestone, and mudstone beds, indicative of palustrine environments periodically influenced by subaerial exposure (Freytet and Verrecchia, 2002). The middle part of the succession comprises palustrine marlstones interbedded with laminated and massive siltstones, while the uppermost part grades into fluvial siltstone facies, including a distinctive pale yellowish-orange laminated siltstone marker horizon that provides stratigraphic correlation with the İncigez and Bozköy sections. Desiccation cracks occur in greenish-grey marlstones and reddish-brown paleosol horizons, whereas parallel laminations are common in the siltstones.

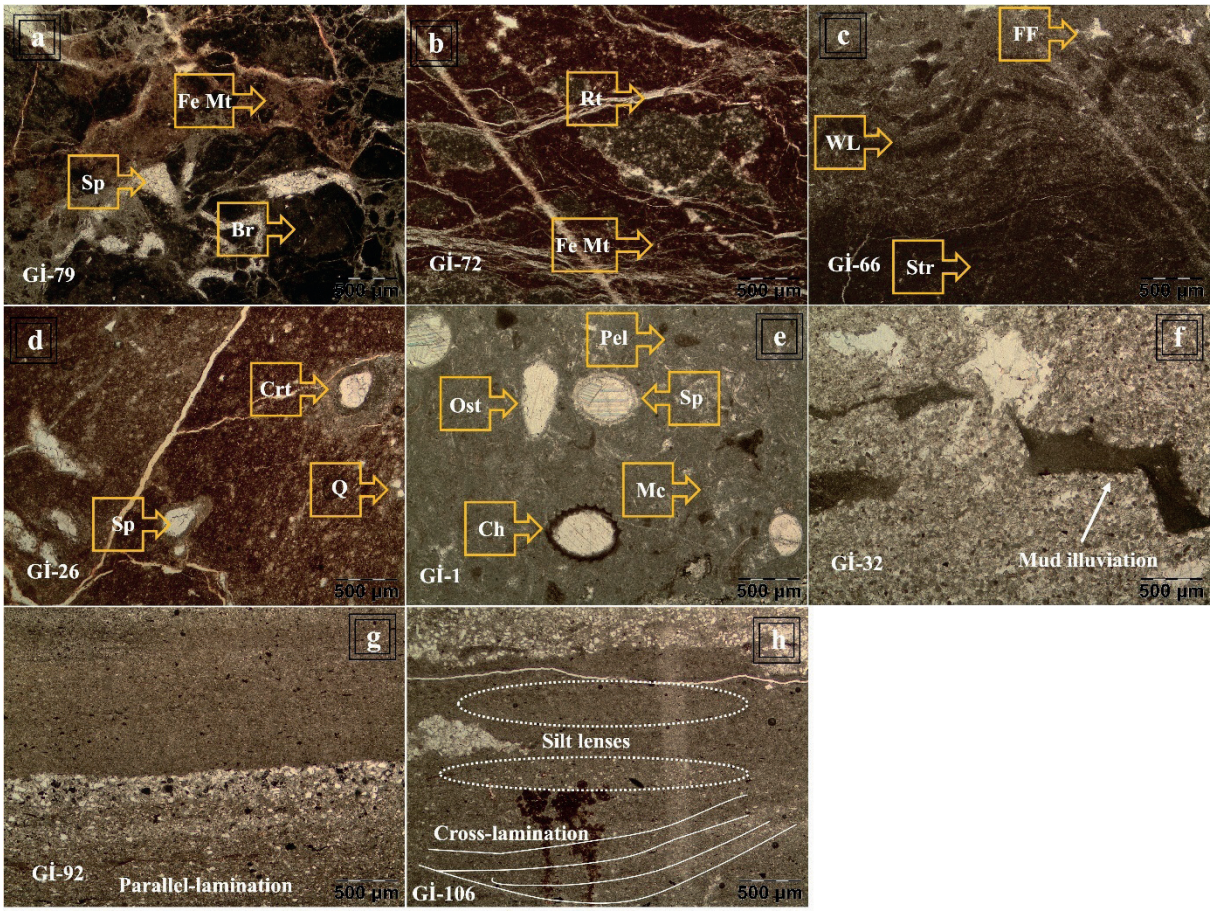

Figure 17. Photomicrographs of thin sections from various lithofacies. Palustrine limestone lithofacies include **(a)** mottled limestone with desiccation cracks and Fe mottling (GI-79, PPl ×4), **(b)** limestone with root cavities (GI-72, PPl ×4), **(c)** laminar calcrete (stromatolite) (GI-66, PPl ×4), and **(d)** green to brown marlstone (GI-26, PPl ×4). The lacustrine limestone microfacies consist of **(e)** ostracod- and charophyte-bearing vaketaşı/biomicrite (GI-1, PPl ×4). Fluvial lithofacies include **(f)** silcrete (GI-32, PPl ×4), **(g)** laminated siltstone (GI-92, PPl ×4), and **(h)** cross-laminated siltstone (GI-106, PPl ×4). Abbreviations: sparry calcite (Sp), mud illuviations (MI), quartz (Q), Fe mottling (Fe mt.), cylindirical root tubes (Crt), stromatolite (Str), wavy lamina (WL), fenestral fabric (FF), root traces (Rt) and, breccias (Br), ostracods (Ost), charophyts (Ch), pellet/peloid (Pel), micrite matrix (Mc).

Şekil 17. *Farklı litofasiyeslere ait ince kesit mikrofotoğrafları. Palüstrin kireçtaşı litofasiyesi şunları içermektedir;* ***(a)*** *kuruma çatlakları ve Fe beneklenmesi gösteren benekli kireçtaşı (GI-79, PPl ×4),* ***(b)*** *kök boşluklu kireçtaşı (GI-72, PPl ×4),* ***(c)*** *laminalı kalker (stromatolit) (GI-66, PPl ×4),* ***(d)*** *yeşilden kahverengiye marn çamurtaşı (GI-26, PPl ×4). Laküstrin kireçtaşı mikrofasiyesi;* ***(e)*** *ostrakod ve karofit içeren vaketaşı/biyomikrit (GI-1, PPl ×4). Flüvyal litofasiyesi;* ***(f)*** *silkrit (GI-32, PPl ×4),* ***(g)*** *laminalı silttaşı (GI-92, PPl ×4),* ***(h)*** *çapraz laminasyonlu silttaşı (GI-106, PPl ×4). Kısaltmalar: sparit (Sp), çamur birikimi (MI), kuvars (Q), Fe boyaması (Fe mt.), silindirik kök tüpü (Crt), stromatolit (Str), dalgalı lamina (WL), fenestral doku (FF), kök izleri (Rt) and, breşleşme (Br), ostrakod (Ost), karofit (Ch), pellet/peloid (Pel), ve mikrit matriks (Mc).*

Petrographic observations reveal:

- Pedogenic and groundwater calcretes with alveolar-septal structures, micritic matrix, root traces, and cement-filled voids (Figure 18a).
- Rooted limestones containing vertical root tubes, intraclasts, and intense bioturbation (Figure 18b).
- Brecciated limestones showing irregular micritic nodules, fenestral fabrics, sparry calcite cement, and evidence of repeated exposure–rewetting episodes (Figure 18c).
- Mottled limestones with silt- to medium-sand-sized quartz grains, intraclasts, Fe-mottling, and sparry calcite-filled desiccation cracks (Figure 18d).
- Fluvial siliciclastic facies comprising micaceous mudstones and siltstones with laminated intervals, fining-upward grading, silt lenses, and cross-laminations (Figure 18e).

The carbonate facies represent mature pedogenic overprinting of lacustrine-margin sediments, whereas the siliciclastic facies record episodic fluvial influx during floodplain aggradation. The stratigraphic succession exhibits a clear shallowing-upward trend from low-energy palustrine carbonates to floodplain siltstones. Alternating mudstone–siltstone and carbonate–paleosol couplets reflect climatically driven wetting–drying cycles along the lake margin, while laminated calcisiltite–mudstone alternations suggest periodic suspension settling and detrital influx under episodically stratified conditions.

Başköy-2 section

The Başköy-2 stratigraphic section is mainly composed of alternating sandstone and mudstone facies, indicating deposition under high-energy channel and lower-energy floodplain conditions.

- Quartz arenite facies composed of >95% polycrystalline volcanic quartz grains, moderately sorted and rounded, well-cemented, and matrix-poor, representing traction-dominated channel deposits formed under high-velocity flows (Figure 19a).
- Quartz wacke facies poorly sorted, angular to subrounded, and rich in muddy matrix, indicating rapid sedimentation during waning flow or channel-margin deposition (Figure 19b).
- Mudstone facies dark red to brownish-black, locally displaying desiccation cracks, Fe-encrustations, and pedogenic textures, reflecting subaerial exposure and soil formation on the floodplain during dry phases (Figure 19c).

The facies association records a transition from point-bar to overbank deposits, characterized by cyclic alternation of sandstone and mudstone units. The basal part is dominated by thick quartz arenite beds that grade upward into thinner quartz wacke and overbank mudstones. This fining- and thinning-upward succession reflects progradational stacking produced by lateral accretion, channel migration, and periodic abandonment. The presence of cross-bedding, normal grading, desiccation cracks, and Fe-mottled horizons indicates alternating fluvial deposition and subaerial exposure consistent with seasonally fluctuating water tables in a low-gradient meandering system.

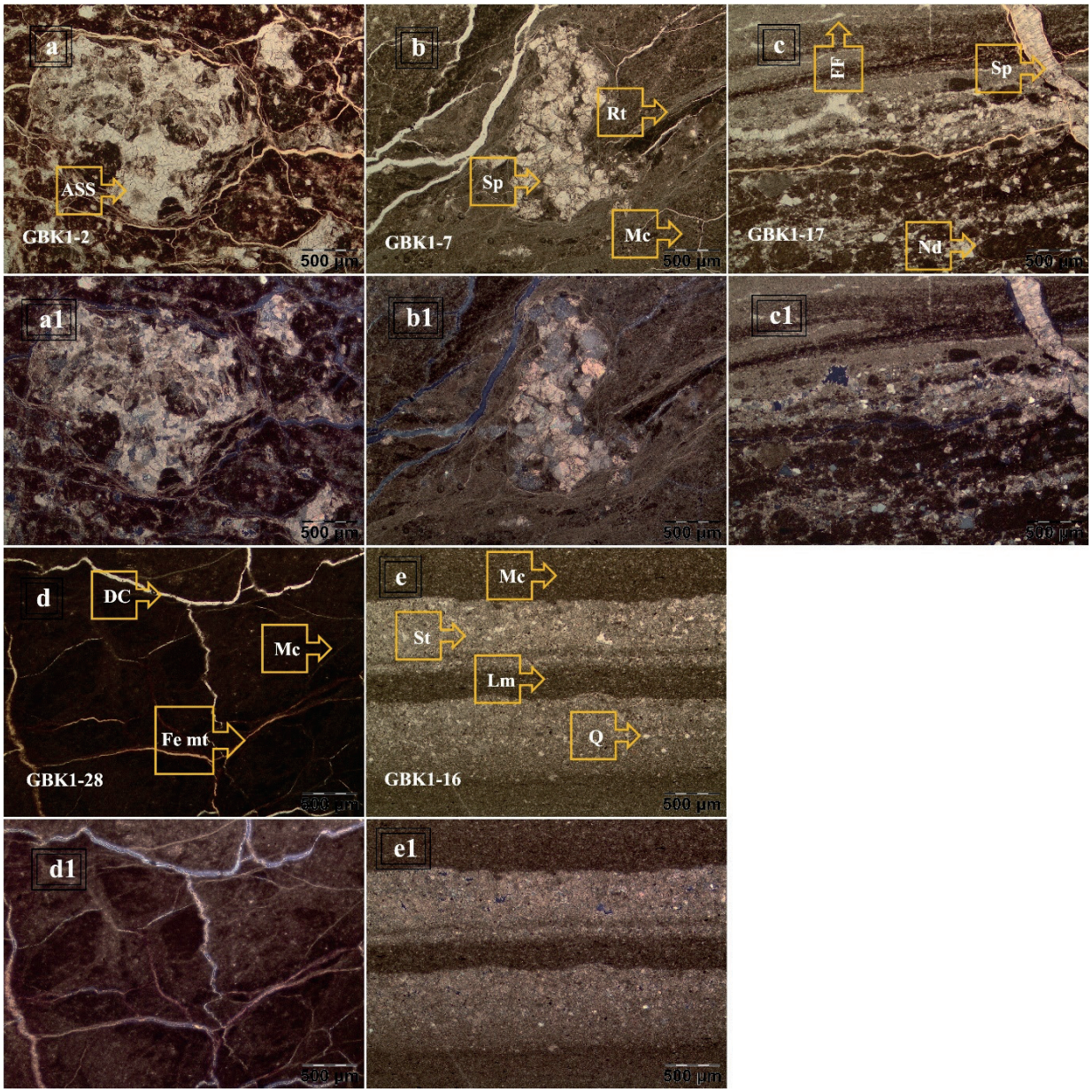

Figure 18. Photomicrographs of thin sections: **(a)** pedogenic and groundwater calcrete (GBK1-2, PPl x4), **(b)** limestone with root cavities (GBK1-7, PPl x4), **(c)** nodular and brecciated limestone (GBK1-17, PPl x4), **(d)** mottled limestone (GBK1-28, PPl x4), and **(e)** laminated siltstone-mudstone (GBK1-16, PPl x4.). Abbreviations: siltite (St.), desiccation cracks (DC), quartz (Q), Fe-mottling (Fe-mt), noduls (Nd), fenestral fabric (FF), alveolar septal structure (ASS), mikrit matriks (Mc).

Şekil 18. *İnce kesitlere ait mikrofotoğraflar;* ***(a)*** *pedojenik ve yeraltısuyu kalkeri* (GBK1-3, PPl x4)*,* ***(b)*** *kök boşluklu kireçtaşı* (GBK1-7, PPl x4), ***(c)*** *nodüllü ve breşleşmiş kireçtaşı* (GBK1-17, PPl x4), ***(d)*** *boyanmış kireçtaşı* (GBK1-28, PPl x4), *ve* ***(e)*** *laminalı silttaşı-çamurtaşı* (GBK1-16, PPl x4). *Kısaltmalar: siltit (St.), kuruma çatlakları (DC), kuvars (Q), Fe boyaması (Fe mt.), nodüller (Nd), fenestral doku (FF), alveollü septal yapı (ASS), mikrit matriks (Mc).*

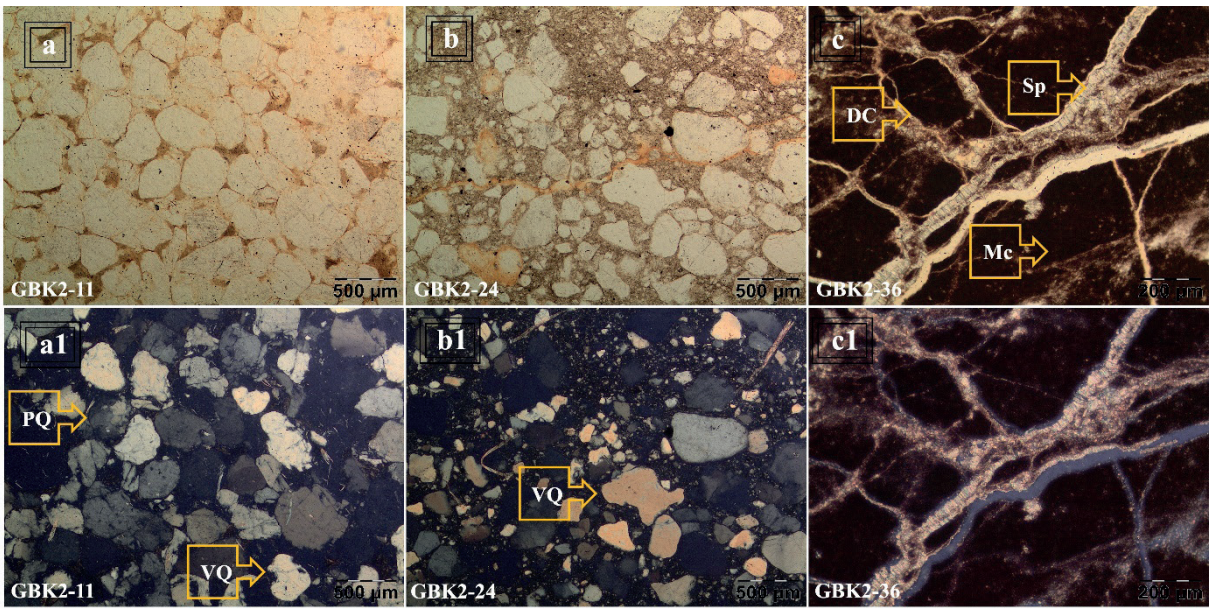

Figure 19. Photomicrographs of thin sections: **(a)** quartz arenite sandstone (GBK2-11, PPl x4), **(b)** quartz wacke sandstone (GBK2-24, PPl x4), and **(c)** mudstone (GBK2-36, PPl x4). Abbreviations: volcanic quartz (VQ.), polycrystalline quartz (PQ.), desiccation cracks (DC.), sparry calcite (Sp.), matrix (Mc.).

Şekil 19. *İnce kesitlere ait mikrofotoğraflar:* ***(a)*** *kuvarsarenit kumtaşı (GBK2-11, PPl x4);* ***(b)*** *kuvarsvake kumtaşı (GBK2-24, PPl x4), ve* ***(c)*** *çamurtaşı (GBK2-36, PPl x4). Kısaltmalar: volkanik kuvars (VQ.), polikristalin kuvars (PQ.), kuruma çatlakları (DC.), sparit (Sp.), matriks (Mc.).*

Başköy-3 section

The Başköy-3 section consists of quartz arenite, quartz wacke, sandy mudstone, and reddish- to blackish-red mudstone lithofacies.

- Quartz arenite facies composed of magmatic, metamorphic, and sedimentary mono- and polycrystalline quartz with minor feldspar and lithic fragments (mica, chert): well-sorted, matrix-poor, and texturally mature, showing syntaxial quartz overgrowths and intergranular porosity (Figures 20a and b).
- Quartz wacke facies moderately to poorly sorted, containing muddy matrix with dispersed feldspar and lithic grains, exhibiting syntaxial quartz overgrowths and partial quartz–calcite cementation (Figure 20c).
- Mudstone facies displaying common root traces, Fe-staining, and sparry calcite-filled desiccation cracks, recording pedogenic overprinting under subaerial exposure (Figure 20d).

The Başköy-3 section exhibits a repetitive fining- and thinning-upward succession, where coarse-grained quartz arenites at the base grade upward into finer quartz wackes and culminate in mudstone horizons. This stacking pattern reflects cyclic point-bar to overbank transitions in a low-gradient meandering system.

Diagenesis

Petrographic analyses of the lacustrine and palustrine carbonate rocks of the Çakrazboz Formation reveal that diagenetic processes played a crucial role in modifying the original depositional fabrics.

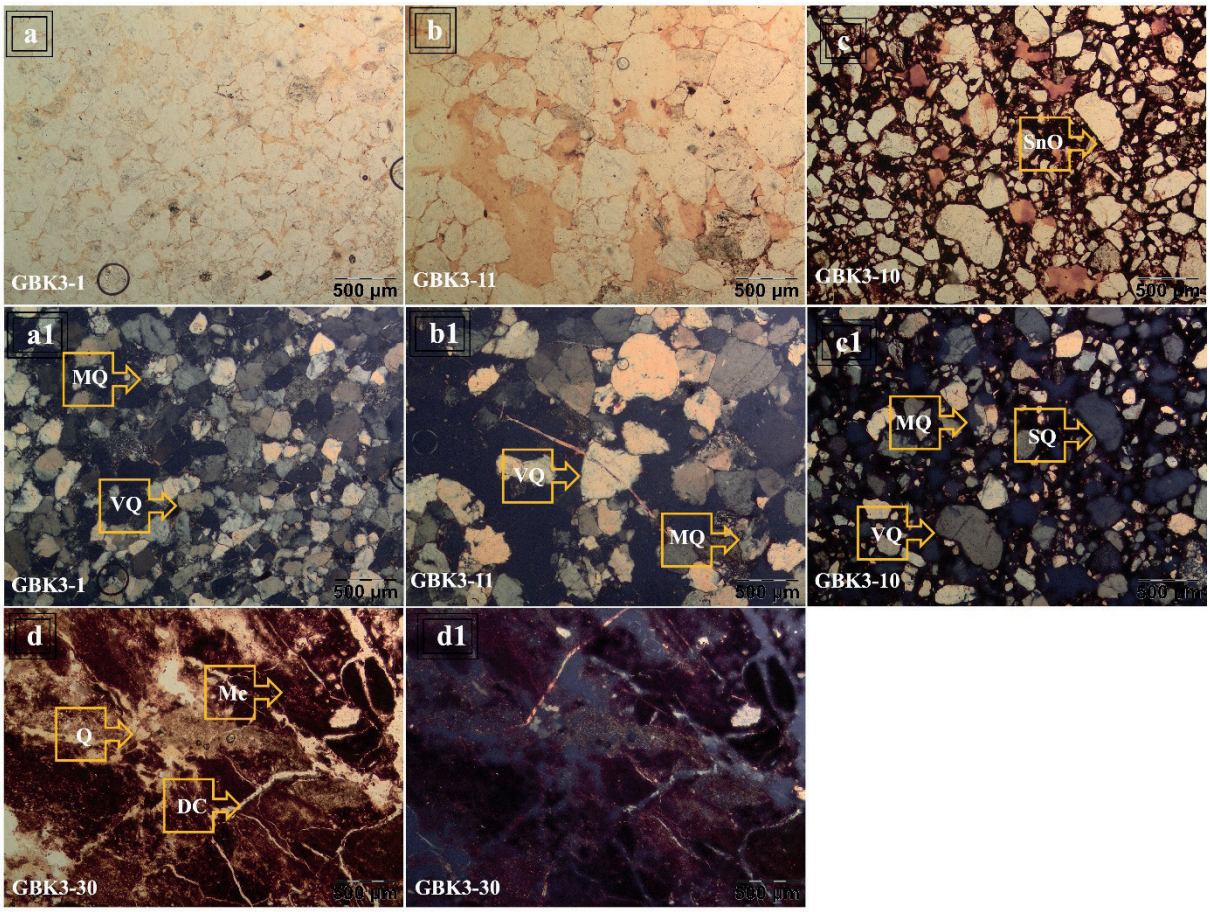

Figure 20. Photomicrographs of thin sections: **(a)** quartz arenite sandstone (GBK3-1, PPl x4), **(b)** quartz arenite sandstone (GBK3-11, PPl x4), **(c)** quartz wacke sandstone (GBK3-10, PPl x4), and **(d)** mudstone (GBK3-30, PPl x4). Abbreviations: magmatic quartz (MAQ.), metamorphic quartz (MQ.), sedimentary quartz (SQ.), syntaxial overgrowth fabric (SnO.), volcanic quartz (VQ.), polycrystalline quartz (PQ.), desiccation cracks (DC.), sparry calcite (Sp.), matrix (Mc.).

Figure 20. *İnce kesitlere ait mikrofotoğraflar;* ***(a)*** *kuvarsarenit kumtaşı (*GBK3-1, PPl x4*),* ***(b)*** *kuvarsarenit kumtaşı (*GBK3-11, PPl x4*),* ***(c)*** *kuvarsvake kumtaşı (*GBK3-10, PPl x4*), ve* ***(d)*** *çamurtaşı (*GBK3-30, PPl x4*). Kısaltmalar: magmatik kuvars* (MAQ.), metamorfik kuvars (MQ.), sedimenter kuvars (SQ.), sintaksiyel üstbüyüme (SnO.), *volkanik kuvars (VQ.), polikristalin kuvars (PQ.), kuruma çatlakları (DC.), sparit (Sp.), matriks (Mc.).*

These processes span the eogenetic, mesogenetic, and telogenetic stages, each leaving distinct mineralogical and textural signatures within the succession (Montañez, and Crossey, 1998; Bustillo et al., 2017).

Eogenetic diagenesis refers to early near-surface alteration under meteoric or lacustrine phreatic–vadose conditions (Tucker, 1990). It includes micritization, early calcite cementation, dissolution, and limited recrystallization soon after deposition. These early fabrics develop in shallow burial settings where pore waters are of low salinity and subject to variable redox conditions (Moore, 1989; Tucker and Bathurst, 1990; Flügel, 2010). Mesogenetic diagenesis takes place during deeper burial and is characterized by compaction, stylolitization, neomorphism, and

pervasive blocky or granular calcite cementation under rising temperature and pressure. These processes reduce primary porosity and produce pressure-solution structures such as stylolites and sutured grain contacts (Mattes and Mountjoy, 1980; Bathurst, 1987; Moore and Wade, 2013; Immenhauser, 2022). Telogenetic diagenesis occurs during uplift and exposure, involving meteoric alteration, dissolution–reprecipitation, calcretization, and karstification in near-surface vadose zones (Tucker, 1990; Wright, 2009; Swart, 2015). Together, these three stages document the progressive post-depositional evolution of the Çakrazboz Formation from shallow burial to subaerial exposure, reflecting the interplay between hydrological changes and climate-driven lake-level oscillations.

In the Çakrazboz section, lacustrine carbonates exhibit irregular fenestral fabrics, stylolites, and pervasive pore-filling by blocky and granular mosaic cements. Microscopic observations show that voids within charophyte oogonia and ostracod shells are filled with sparry calcite, indicating precipitation in meteoric-phreatic to shallow burial settings. Stylolitic seams enriched in Fe-oxides record pressure solution associated with burial compaction (mesogenesis), leading to porosity loss and enhanced sparry calcite cementation.

In the İncigez section, diagenetic features include birdseye and laminoid fenestral fabrics, granular mosaic cements, and nodular–brecciated textures typical of supratidal to intertidal environments periodically exposed to meteoric waters. Calcrete facies display alveolar-septal structures and root-related fabrics, evidencing pedogenic overprinting under semi-arid conditions (Wright and Tucker, 1991). These characteristics correspond to telogenetic alteration linked to repeated subaerial exposure and soil formation (Alonso-Zarza and Wright, 2010).

The Başköy-1 section records complex diagenetic overprinting related to prolonged subaerial exposure and pedogenesis. Early laminoid fenestral fabrics reflect intermittent desiccation in palustrine settings (eogenesis) (Philcox, 1963). Alveolar-septal structures, rhizoliths, and micritic nodules within calcretes indicate strong pedogenic modification and recrystallization under meteoric conditions (telogenesis). Brecciated and nodular limestones, containing fenestral fabrics and sparry calcite cements, developed through alternating wetting–drying cycles and mechanical disruption of semi-lithified sediments. Such features typify pedogenic calcretes and palustrine carbonates formed under fluctuating groundwater tables and semi-arid climatic regimes (Verrecchia, 2000).

An integrated assessment of all sections suggests a diagenetic progression from early eogenetic cementation, through mesogenetic compaction and stylolitization, to telogenetic pedogenic calcretization upon subaerial exposure (Figure 21). As defined by Immenhauser (2022), mesogenetic processes operate within shallow-to-intermediate burial depths (hundreds of meters to a few kilometers), where compaction and fluid–rock interactions dominate. The widespread occurrence of alveolar-septal fabrics, rhizoliths, and calcrete horizons in upper units of the succession highlights intense telogenetic reworking following uplift and basin-margin exposure.

The relationship between diagenesis and facies is primarily controlled by depositional environment, early cementation style, and groundwater composition. Lacustrine facies preserve early micritic and phreatic cements due to sustained water saturation, whereas palustrine and marginal facies exhibit pedogenic features such as alveolar-septal fabrics, rhizoliths, and calcrete crusts linked to telogenetic exposure and soil formation (Verrecchia, 2000; Tucker and Bathurst, 1990).

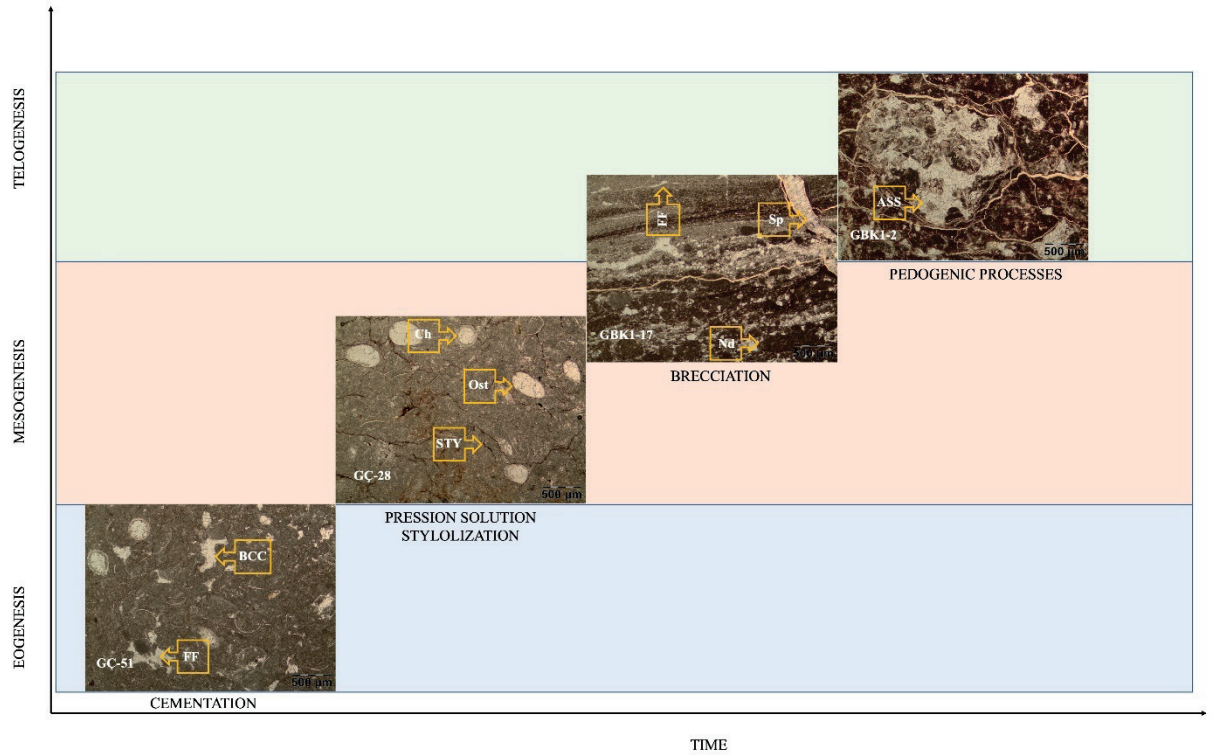

Figure 21. Diagenetic stages vs. time graphic represents diagenetic characteristics of the sedimentary rocks of the Çakrazboz Formation.

Şekil 21. *Diyajenez evreleri-zaman grafiği, Çakrazboz Formasyonu'na ait sedimanter kayaçların diyajenetik özelliklerini göstermektedir.*

Fluctuating lake levels promoted dissolution–reprecipitation cycles, causing brecciation, stylolitization, and nodulation, particularly in upper intertidal to supratidal zones (Armenteros, 2010; Immenhauser, 2022). Consequently, facies architecture exerts a primary control on the spatial distribution, intensity, and style of diagenetic processes within the Çakrazboz Formation, capturing the hydrological and climatic variability of the Late Triassic continental basin.

DISCUSSION

The Çakrazboz Formation presents an integrated record of sedimentary, petrographic, and diagenetic processes that collectively document the evolution of a Late Triassic continental basin along the southern Eurasian margin. The observed facies assemblages, ranging from lacustrine carbonates to fluvial sandstones, capture the spatial and temporal response of depositional systems to climatic, hydrological, and tectonic controls. Variations in lithofacies, color, and diagenetic overprinting across the six measured sections reveal alternating humid and semi-arid conditions that governed lake-level and groundwater fluctuations. These features underscore the sensitivity of continental basins to orbitally paced climatic cyclicity and regional tectonic reorganization during the disassembly of Pangea. Integrating sedimentological and petrographic data with regional paleogeographic reconstructions provides a robust framework for interpreting basin evolution, paleoclimate patterns, and diagenetic transformation within the Western Pontides during the Late Triassic.

Regional Paleogeography, Global Context, and Paleoclimate Reconstructions

During the Triassic, the supercontinent Pangea reached its maximum integrity before gradual fragmentation began. The Cimmeria microcontinent, comprising present-day Türkiye, Iran, Afghanistan, and Tibet, rifted northward from Gondwana, leading to the closure of the Paleotethys Ocean and the opening of the Neotethys Ocean, reshaping the Tethyan realm (Scotese, 2021). In the Early Triassic (ca. 250–245 Ma), the region corresponding to modern Türkiye occupied a position along Gondwana's northern passive margin. By the Middle Triassic (245–235 Ma), rifting intensified and shallow epicontinental seas advanced across the Cimmerian blocks. During the Late Triassic (230–200 Ma), the northward-drifting Cimmeria collided with Eurasia, initiating the early Cimmerian orogeny and final Paleotethys closure (Şengör, 1990; Schettino and Turco, 2011; van Hinsbergen et al., 2020; Scotese, 2021) (Figure 22). These events established the tectonic framework of the Pontides and Taurides as distinct crustal elements along the Neotethyan margin.

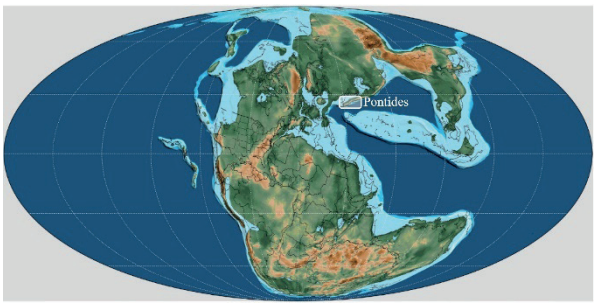

Figure 22. Paleogeographic map of the Rhaetian–Hettangian interval (Late Triassic, ~200 Ma), with the Pontides shown within the shaded area on the map. (Adapted from Scotese et al. (2021).)

Şekil 22. *Resiyen–Hettanjiyen aralığına (Geç Triyas, ~200 Ma) ait paleocoğrafya haritası üzerinde Pontidler gölgelendirilmiş alan içinde gösterilmiştir. (Şekil Scotese vd. (2021)'den uyarlanmıştır.)*

Global paleogeographic reconstructions (Golonka, 2007; Robertson et al., 2016; Scotese and Schettino, 2017) indicate that the Turkish terranes, including the Sakarya Continent (İstanbul–Zonguldak and Sakarya zones), the Kırşehir Block, and the Tauride–Anatolide platform, occupied paleolatitudes of approximately 25°S to 35°S during the Middle to Late Triassic, within the subtropical arid to semi-arid belt of the Southern Hemisphere. The Sakarya Continent constituted the northern segment of the Cimmerian microplate system and had already been detached from Gondwana, whereas the Kırşehir and Tauride–Anatolide blocks remained positioned close to the actively extending Neotethyan margin. This paleogeographic configuration explains the coexistence of continental red-bed and lacustrine successions in northern Türkiye and widespread carbonate platforms farther south (Robertson et al., 2006). By the Ladinian–Carnian (ca. 242–227 Ma), progressive rifting produced alternating marine seaways and continental basins along the Cimmerian margin, reflecting a gradient from continental interiors in the north to open-marine settings in the south within a back-arc extensional system (Golonka, 2007).

The Triassic climate resulted from the coupling of atmospheric, oceanic, and continental systems that governed global energy and moisture exchange (Raynaud et al., 1993; Zielinski, 1995). According to global paleoclimate models (Boucot et al., 2013; Scotese, 2021), the Early Triassic experienced extreme greenhouse conditions with high CO_2 levels and widespread aridity following the end-Permian mass extinction. During the Middle Triassic, monsoonal circulation introduced episodic humidity to the subtropical Tethyan belt, and by the Late Triassic, a highly seasonal semi-arid climate prevailed. Such variability favored the accumulation of fluvial–lacustrine successions and red-bed siliciclastic deposits in interior basins of the Cimmerian terranes (Figure 23).

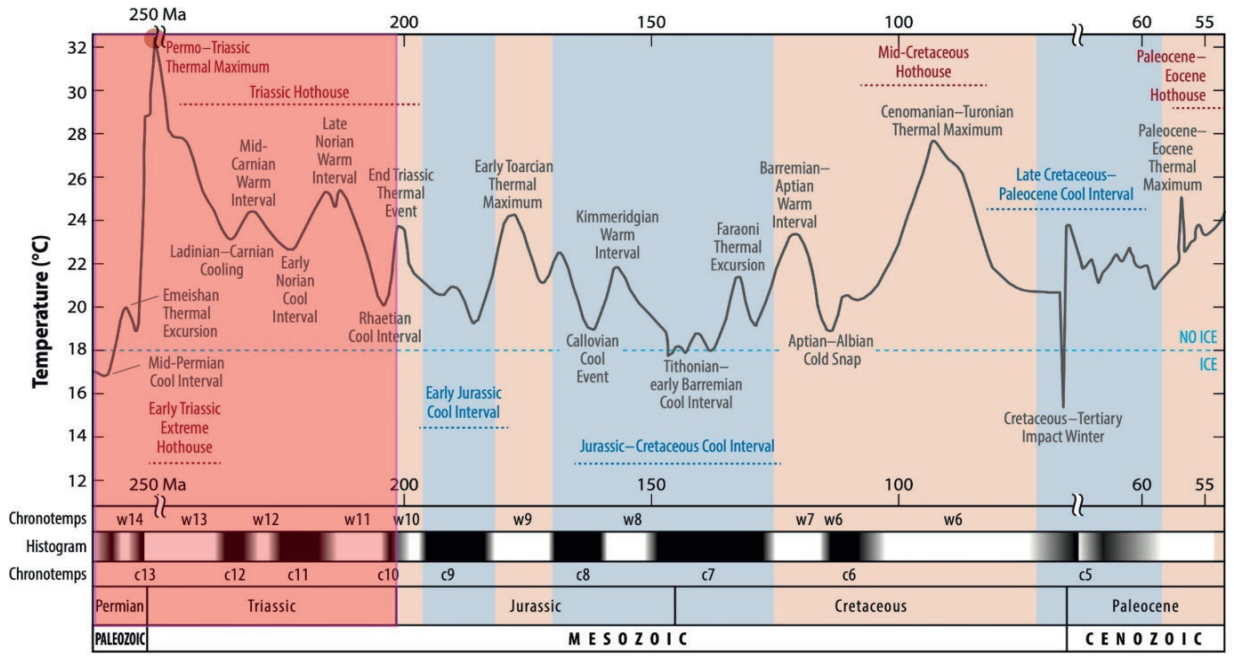

Figure 23. Mesozoic paleotemperature timescale showing warm intervals (white) and cool intervals (black). During the Early Triassic, global temperatures reached extreme hothouse conditions of ~32 ºC, subsequently decreasing to ~24 ºC by the Late Triassic. The Early–Late Triassic interval contains two warm and three cool phases. Following the Rhaetian, temperatures rose from ~19 ºC to ~24 ºC during the end-Triassic thermal event. The solid grey curve represents the Global Average Temperature, while the chronostratigraphic framework follows the International Chronostratigraphic Chart (2020/01) (Figure adapted from Scotese et al. (2021)).

Şekil 23. *Mesozoyik paleosıcaklık zaman ölçeğinde sıcak dönemler beyaz, serin dönemler siyah ile gösterilmektedir. Erken Triyas'ta küresel sıcaklıklar yaklaşık 32 ºC ile aşırı sıcak (extreme hothouse) koşullara ulaşmış, Geç Triyas'a gelindiğinde ise yaklaşık 24 ºC'ye düşmüştür. Erken–Geç Triyas aralığı, toplamda iki sıcak ve üç serin evre içermektedir. Rhaetiyen sonrasında, End-Triyas termal olayı sırasında sıcaklıkların yaklaşık 19 ºC'den 24 ºC'ye yükseldiği görülmektedir. Gri eğri küresel ortalama sıcaklığı göstermekte olup zaman ölçeği International Chronostratigraphic Chart (2020/01) temel alınarak düzenlenmiştir (Şekil Scotese vd. (2021)'den uyarlanmıştır.).*

Across Pangea, reduced shelf areas and enhanced continentality strengthened monsoonal precipitation gradients (Haq et al., 1987; Rafferty, 2010). These gradients were further modulated by orbital forcing, particularly Earth's precessional cycle. According to the symmetric monsoon model proposed by Kutzbach (1994), maximum precipitation in the Late Triassic Northern Hemisphere occurred near the summer solstice (June–August), corresponding to perihelion. During these intervals, intensified solar radiation increased evaporation from the Tethyan Ocean, enhancing northward moisture transport and precipitation over continental interiors. Aphelion summers were marked by lower insolation and weaker monsoonal circulation, resulting in drier climates, intensified oxidation, and episodic lake desiccation (Vollmer et al., 2008). These orbitally forced fluctuations governed the hydrological balance within the Çakrazboz Basin, producing the cyclic lacustrine-palustrine-fluvial architecture that typifies the formation.

Quantitative paleotemperature reconstructions (Scotese et al., 2021) estimate global mean surface temperatures of ~20 ± 2 ºC, with tropical seas near 30 ºC and weak latitudinal gradients (~0.25–0.30 ºC). Under such greenhouse conditions, the Turkish terranes experienced alternating arid and

humid phases, producing cyclic oxidized and reduced facies. Pedogenic calcretes, root traces, and desiccation cracks indicate arid intervals, whereas greenish-grey marls and lacustrine carbonates represent humid phases with high groundwater levels (Platt and Wright, 1992; Cecil, 1990; Verrecchia, 2007; Alonso-Zarza and Wright, 2010).

Lacustrine systems are particularly sensitive to climatic fluctuations, with lake-level variations serving as key paleoclimate proxies (Adrian et al., 2009; Argyilan and Forman, 2003). In the Çakrazboz Formation, reddish-brown marlstones record arid intervals, while greenish-grey marls indicate more humid conditions associated with enhanced groundwater recharge and flooding of lake margins during wet phases of precessional cycles. Facies architecture within the formation supports a temperate to subhumid climate regime: alternating fluvial, palustrine, and lacustrine facies reflect cyclical changes in precipitation and evaporation (Figure 24).

Bioturbated limestones rich in ostracods and charophytes, micritic carbonates, and greenish-grey mudstones indicate well-oxygenated lake waters and warm and humid conditions conducive to carbonate productivity. Palustrine facies show brecciation, fenestral fabrics, and shrinkage cracks, recording repeated wetting–drying cycles, while pedogenic features such as rhizoliths and alveolar-septal structures indicate prolonged subaerial exposure under seasonally arid conditions. The occurrence of pedogenic and groundwater calcretes, coupled with alternating green and brown marlstones, suggests periodic shifts between groundwater-fed wetlands and oxidizing ephemeral lake settings (Wright and Tucker, 1991; Tucker and Sparks, 2024). As noted by Platt and Wright (1992), carbonate precipitation in lacustrine systems is favored under semi-arid to subhumid climates, where carbonate-saturated solutions may derive from both surface runoff and groundwater influx (De Wet et al., 1998; Gvirtzman, 2006).

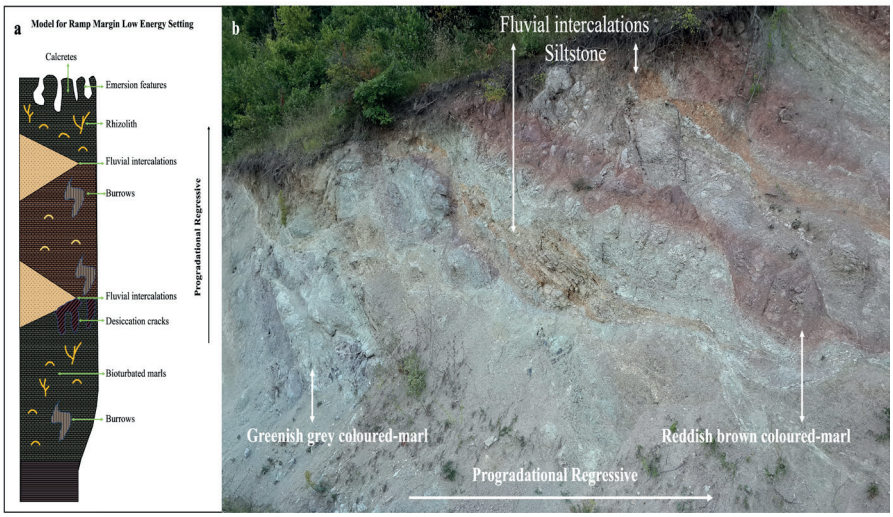

Figure 24. a) Conceptual model illustrating a low-energy ramp-margin depositional setting developed under orbitally driven climatic cyclicity (sketch adapted from Alonso-Zarza and Tanner, 2009), **(b)** Representative field photograph from the İncigez section showing the characteristic lithofacies of the Çakrazboz Formation that typify this low-energy ramp-margin depositional system.

Şekil 24. a) *Yörünge kaynaklı iklim döngüleri altında gelişen düşük enerjili rampa-kenarı çökelme ortamını gösteren kavramsal model (Alonso-Zarza ve Tanner, 2009'dan uyarlanmıştır),* ***(b)*** *İncigez kesitinden alınmış, Çakrazboz Formasyonu'nun bu düşük enerjili rampa-kenarı çökelme sistemini karakterize eden başlıca litofasiyeslerini gösteren temsilî arazi fotoğrafı.*

Color variations within the marlstones correspond to redox fluctuations in the lake water column, reflecting oscillations in pH and Eh. Detailed color-based facies analysis using the GSA Rock-Color Chart (2009) (Figure 25) indicates that light greenish-grey (5GY 7/1) and olive grey (5Y 5/2) tones formed under reducing to weakly reducing conditions in profundal to sublittoral zones, whereas whitish carbonates (N9) reflect well-oxygenated shallow-lake environments. Palustrine facies with dark yellowish-brown (5YR 4/4) and greyish-black (N2) hues correspond to alternating oxidizing and reducing phases during subaerial exposure and groundwater saturation. Fluvial facies displaying yellowish-grey (10YR 7/2), dark reddish-brown (2.5YR 3/6), and blackish-red (10R 3/4) colors indicate well-drained and oxidizing channel fills and seasonally dry floodplains enriched in iron oxides (Table 4). The stratigraphic alternation of oxidized and reduced facies therefore aligns with precessional to eccentricity-scale climate cycles, where wet phases promoted reducing lacustrine–palustrine conditions and dry phases enhanced oxidation in exposed floodplain and lake-margin deposits.

These features align with the limno-eustatic model of Wagreich et al. (2014), which links lake-level variations to groundwater storage during greenhouse climates. High groundwater levels during wet periods correspond to deeper lakes and regional sea-level lowstands (Sames et al., 2020). Thus, the rhythmic alternation of oxidized and reduced marls, desiccation cracks, and paleosols records hydrological cycles modulated by orbital forcing and climate-induced groundwater fluctuations (Glenn and Kelts, 1991). By the end of the Triassic, convergence of the Cimmerian blocks with Eurasia caused regional uplift and basin compartmentalization, leading to widespread subaerial exposure and the deposition of fluvial, palustrine, and lacustrine successions in the Western Pontides (Golonka, 2007; Robertson et al., 2016).

Facies Type	**Color (GSA Name & Munsell Code)**	**Redox Condition**	**Lake Type / Environment**
Lacustrine (Profundal to Sublittoral)	Light greenish grey (5GY 7/1), Olive grey (5Y 5/2)	Reducing to weakly reducing	Underfilled to balanced-fill profundal–sublittoral lake zones
Lacustrine (Shallow)	White (N9)	Well-oxygenated	Well-oxygenated shallow lacustrine settings
Palustrine	Dark yellowish brown (5YR 4/4), Greyish black (N2)	Alternating oxidizing/reducing	Groundwater-saturated marshes; episodic subaerial exposure
Fluvial (Channel fills, floodplains)	Yellowish grey (10YR 7/2), Dark reddish brown (2.5YR 3/6), Blackish red (10R 3/4)	Oxidizing	Well-drained channels and seasonally dry floodplains

Figure 25. Facies color codes (GSA Rock-color chart, 2009), redox conditions, and lake types.
Şekil 25. *Fasiyes renk kodları (*GSA Rock-color chart, 2009), indirgenme koşulları ve göl tipleri.

Table 4. Facies colors of the Çakrazboz Formation, their corresponding GSA Rock-Color Chart (2009) codes, associated oxidation/reduction conditions, and possible paleoenvironmental interpretations.

Çizelge 4. *Çakrazboz Formasyonu'na ait fasiyes renkleri, bunlara karşılık gelen GSA Kaya-Renk Çizelgesi (2009) kodları, ilişkili oksidasyon/redüksiyon koşulları ve olası paleoçevresel yorumları.*

Facies Type	GSA Rock-Color Chart (2009) Code	Color description	Oxidation/Reduction Condition	Possible Paleoenvironmental Interpretation
Lacustrine	5GY 7/1	Light greenish grey	Reduction	Deep lake bottom, low-oxygen, reducing conditions
Lacustrine	5Y 5/2	Olive grey	Weak reduction	Intermediate depth, semi-reducing lake bottom
Lacustrine	N9	Whitish	Neutral/Oxic	Carbonate-rich, well-oxygenated shallow lake environment
Palustrine	5YR 4/4	Dark yellowish brown	Oxidation	Surface oxidation during dry phases, lake-margin marsh
Palustrine	N2	Greyish black	Reduction	Marsh bottom, saturated, anaerobic conditions
Palustrine	2.5Y 5/2	Greenish grey	Weak reduction	Groundwater-influenced, marsh environment
Fluvial	10YR 7/2	Yellowish grey	Oxidation	Well-drained, high-energy channel fill
Fluvial	2.5YR 3/6	Dark reddish brown	Oxidation	Floodplain, well-oxygenated conditions
Fluvial	10R 3/4	Blackish red	Oxidation	Iron oxide-rich, seasonally dry floodplain

Consequently, the Late Triassic climate of the Western Pontides was governed by monsoonal dynamics within the southern mid-latitudes of Pangea, where the interplay between tectonic subsidence, sediment supply, and orbitally forced climatic oscillations controlled the hydrological balance of the Çakrazboz Basin, producing its characteristic cyclic facies architecture and a detailed record of continental climate variability during the fragmentation of Pangea.

Depositional Environments and Hydrological Variability

Sedimentological, petrographic, and stratigraphic evidence from the Çakrazboz Formation indicates deposition within a predominantly balanced-fill lacustrine basin (Carroll and Bohacs, 1999; Bohacs et al., 2000), punctuated by intervals reflecting underfilled and overfilled hydrological states, as described by Zavala et al. (2024). This variability highlights the influence of orbitally paced climatic oscillations, fluctuating sediment supply, and hydrological connectivity on basin evolution.

Within the framework of Bohacs et al. (2000), the Çakrazboz Formation exhibits the principal characteristics of a balanced-fill lake system: a dynamic equilibrium between sediment and water influx, vertical facies successions recording alternations between profundal, sublittoral, and marginal environments, and redox-sensitive marl color changes linked to groundwater fluctuations. Laminated to massive carbonate mudstones and alternating wackestone–packstone microfacies in the Çakrazboz section reflect low-energy profundal to sublittoral lacustrine deposition. The laminated carbonate mudstones, with fine stratification and limited bioturbation, record dysoxic to anoxic bottom-water conditions, while wackestone–packstone couplets containing ostracods, charophytes, peloids, and pellets represent moderate-energy sublittoral zones. Alternations between these microfacies are interpreted as lake-level fluctuations typical of balanced-fill systems.

Palustrine and marginal lacustrine limestones interbedded with green to brown marls –

observed in the Bozköy, Başköy-1, and upper İncigez sections – were deposited in vegetated swampy areas along shallow lake margins or

distal alluvial plains (Alonso-Zarza, 2003). The presence of root traces, alveolar-septal fabrics, and fenestral textures indicates pedogenic overprinting, consistent with meteoric diagenesis in subaerially exposed environments (Tucker and Bathurst, 1990). Pedogenic features, microbial textures, and green–brown marl transitions indicate alternating oxidation–reduction conditions driven by groundwater-table fluctuations, consistent with the balanced-fill model. Periodic subaerial exposure during regression and re-flooding during transgression produced palustrine fabrics and repetitive shallowing-upward cycles (see Figure 26 for the depositional model).

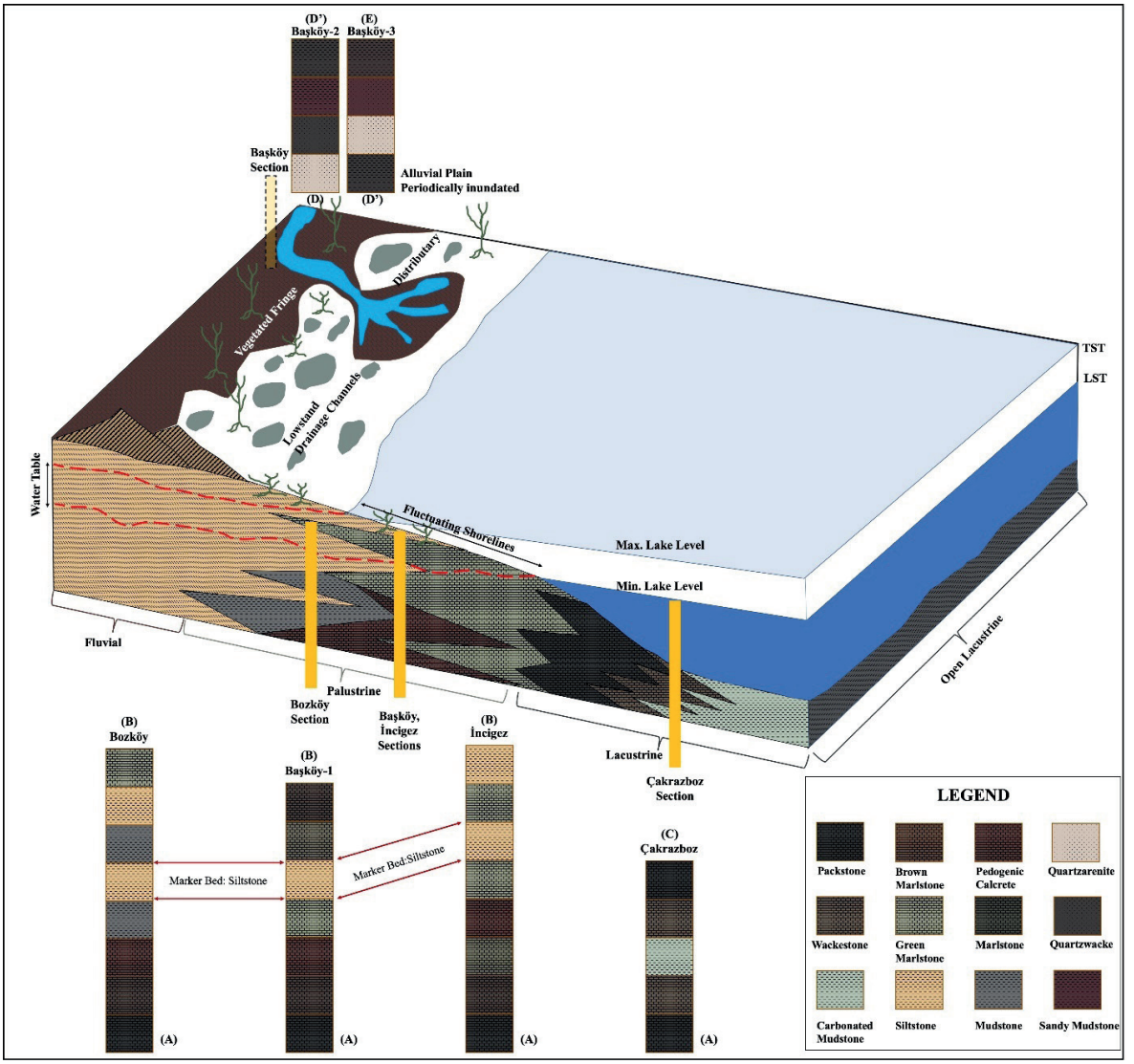

Figure 26. Depositional model of the study area illustrating the spatial and environmental context of the Çakrazboz Formation. The model reflects a balanced-fill lake basin characterized by alternating fluvial, palustrine, and lacustrine depositional systems.

Şekil 26. *Çalışma alanına ait çökelme modeli; Çakrazboz Formasyonu'nun çökelim ortamını ve fasiyeslerin mekânsal dağılımını göstermektedir. Model, flüvyal, palüstrin ve gölsel çökel sistemlerin ardalanmasıyla karakterize edilen dengeli dolgu (balanced-fill) tipi bir göl havzasını yansıtmaktadır.*

To establish lateral continuity among the measured sections, a distinctive pale yellowish-orange colored laminated siltstone beds was identified and traced as a marker horizon across the study area. This laterally persistent layer provides a reliable stratigraphic reference for correlating individual sections and reconstructing the basin-scale facies architecture (Figure 27).

When assessed through the hydrological classification of Zavala et al. (2024), the Çakrazboz Formation records recurrent alternations between three lake types:

- Underfilled conditions in the lower İncigez, Çakraz, and Başköy-2 and -3 sections, where profundal carbonates or fluvial–supratidal deposits with fining- and thinning-upward trends, pedogenic calcretes, mud cracks, and subaerial exposure features developed in closed settings.
- Balanced-fill conditions in the upper İncigez and Başköy-1 sections, where fining-upward transgressive intervals are overlain by coarsening-upward progradational littoral deltas, indicating that lake level reached the spill point before regressive delta progradation.
- Overfilled conditions in Bozköy and parts of Başköy-1, where thickening- and coarsening-upward successions indicate prolonged freshwater inflow in open systems (Figure 28).

The Başköy-2 and Başköy-3 sections show meandering fluvial point-bar successions with fining-upward sequences of conglomerates, sandstones, siltstones, and mudstones, and sedimentary structures such as cross-bedding, ripple laminations, flaser and wavy bedding, mud cracks, and root traces. These successions represent proximal alluvial to marginal lacustrine environments feeding the basin. The sedimentological and petrographic characteristics collectively indicate deposition within a low-gradient, meandering fluvial system periodically influenced by floodplain and marginal lacustrine processes. The predominance of subangular to subrounded quartz grains, poor to moderate sorting, and variable sphericity values (0.25–0.70) indicates short-distance sediment transport under fluctuating hydraulic regimes, consistent with a semi-arid climatic setting. These features, together with fining-upward successions, erosional basal contacts, and pedogenically modified overbank mudstones, suggest deposition in channel–point bar to floodplain environments formed by lateral channel migration and episodic flooding. In the Başköy-3 section, reddish pedogenically mottled mudstones, crevasse-splay sandstones, and thin palustrine limestones record intermittent lacustrine incursions, implying transient hydrological connections between fluvial channels and shallow lakes at the basin margin.

Textural parameters plotted on the Stewart (1958), Friedman (1961), Miola and Wesser (1968), and Passega (1964) diagrams further support deposition by fluvial processes, where sediment was transported as both bedload and suspension load under variable flow conditions. Provenance data based on Dickinson's (1985) QFL ternary diagram show that the Başköy sandstones plot within the craton-interior field, indicating derivation from a stable continental source dominated by quartz-rich detritus. This provenance signature, together with the low compositional and textural maturity of the sandstones, implies limited sedimentary recycling and rapid delivery from proximal upland sources along the basin margin. These results confirm that the Başköy-2 and Başköy-3 successions represent the proximal fluvial input systems of the Çakrazboz Basin, supplying detritus to the balanced-fill lacustrine depocentre and recording climatic oscillations that alternated between wet and dry phases during the Late Triassic.

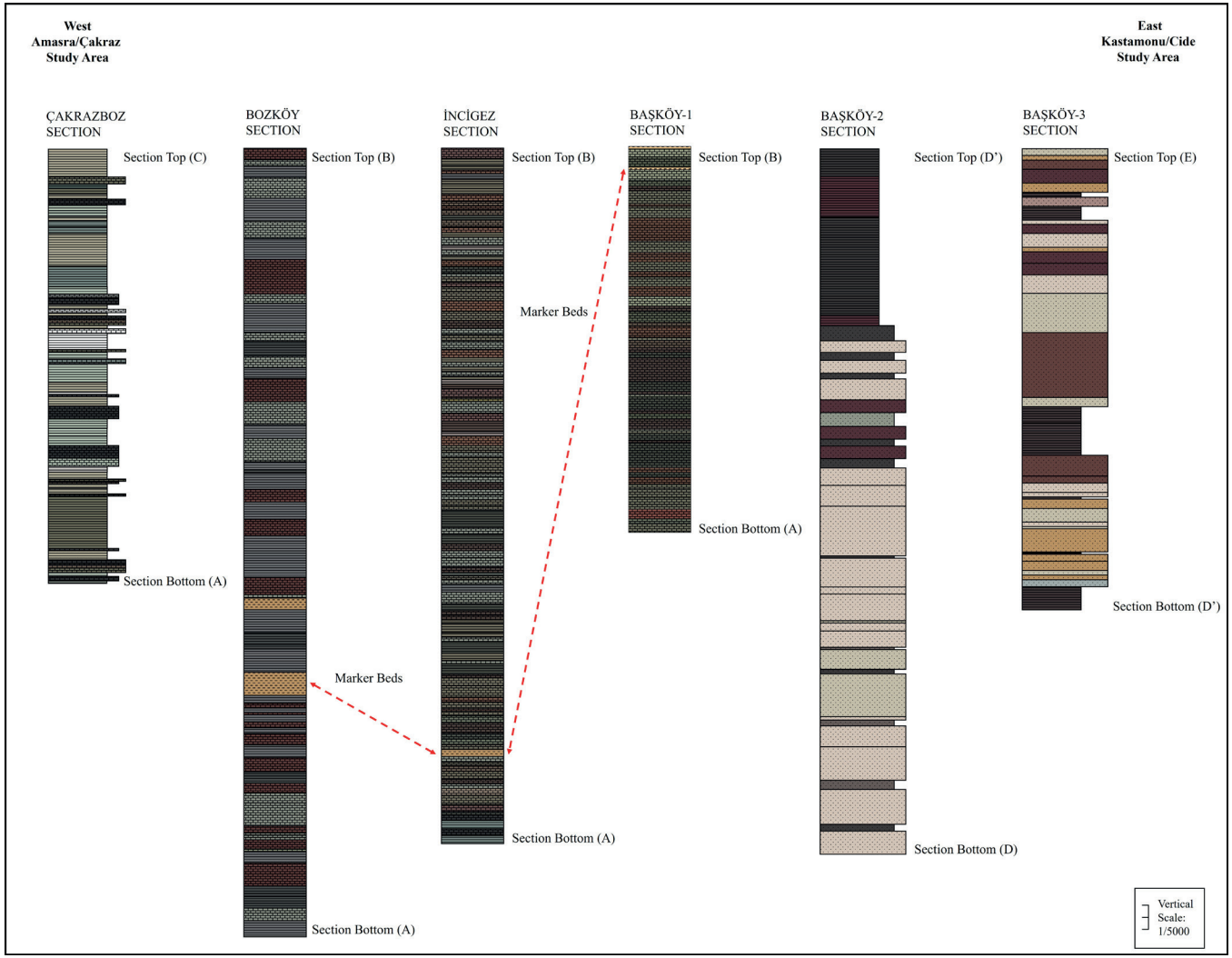

Figure 27. Lithostratigraphic correlation of the measured stratigraphic sections of the Çakrazboz Formation within the vertical succession. Correlation is based on lithofacies characteristics, vertical stacking patterns, and key stratigraphic marker beds.

Şekil 27. *Çakrazboz Formasyonu'na ait ölçülmüş stratigrafik kesitlerin düşey istif içerisindeki litostratigrafik korelasyonu. Korelasyon; litofasiyes özellikleri, düşey istiflenme desenleri ve ayırt edici stratigrafik belirleyici tabakalar temel alınarak yapılmıştır.*

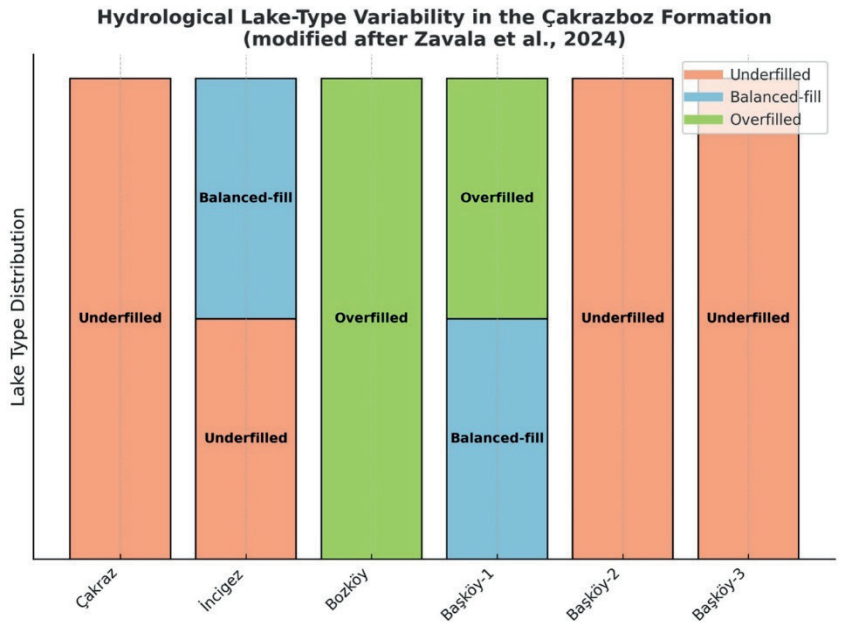

Figure 28. Hydrological lake-type variability in the Çakrazboz Formation.
Şekil 28. *Çakrazboz Formasyonu'nda hidrolojik göl tipi değişkenliği.*

In addition to these sedimentological features, diagenetic observations further refine the interpretation of depositional environments. Lacustrine carbonates from the Çakrazboz and İncigez sections preserve eogenetic features such as micritization, early cementation, and partial compaction, while palustrine and marginal facies display meteoric alteration, brecciation, and calcrete formation typical of telogenetic diagenesis (Flügel, 2010; Alonso-Zarza and Wright, 2010; Tucker and Sparks, 2024). Such diagenetic overprinting, coupled with rhythmic facies alternation, points to repeated cycles of subaerial exposure and flooding under semi-arid climatic conditions.

Overall, the depositional system of the Çakrazboz Formation, though primarily balanced-fill, oscillated between underfilled and overfilled stages, reflecting climate-controlled cyclicity and variable sediment–water budgets. The alternation of oxidized (reddish-brown) and reduced (greenish-grey) marl beds, desiccation cracks, and paleosol horizons records hydrological and climatic cycles consistent with semi-arid monsoonal variability during the Late Triassic. This dynamic evolution parallels other Western Tethyan continental basins (e.g., northern Italy, Austria, and South China), where alternating lacustrine and fluvial regimes similarly document orbitally forced climatic oscillations during the fragmentation of Pangea. Thus, the Çakrazboz Formation provides a valuable record of Late Triassic continental sedimentation in the Western Pontides, capturing the interplay between climate, hydrology, diagenesis, and tectonics during the early stages of Pangea's disintegration

CONCLUSION

The sedimentological and petrographic analyses of the Çakrazboz Formation yield the following key conclusions:

Depositional dynamics: The Çakrazboz Formation represents a Late Triassic balanced-fill lacustrine basin that periodically alternated between underfilled, balanced-fill, and locally overfilled hydrological states. These transitions reflect variable sediment–water influx and basin connectivity in response to orbitally paced climatic oscillations.

Facies evolution: Underfilled stages are marked by profundal carbonate or fluvial–supratidal successions (Çakraz, lower İncigez, Başköy-2, Başköy-3), whereas balanced-fill stages show transgressive–regressive cycles with littoral progradation (upper İncigez, Başköy-1). Overfilled stages, recorded in Bozköy and upper Başköy-1, developed under open hydrological conditions with persistent freshwater inflow and deltaic progradation.

Paleoclimate control: Color variations, diagenetic imprints, and paleosol horizons indicate that lake-level fluctuations were controlled by precessional and eccentricity-scale climate forcing, consistent with monsoonal variability reconstructed for the global Late Triassic greenhouse world (Boucot et al., 2013; Scotese, 2021).

Regional implication: The Çakrazboz Formation captures the response of Western Pontide continental basins to orbitally modulated hydrological shifts within a semi-arid to subhumid subtropical belt along the Cimmerian margin. Its cyclic sedimentation pattern parallels coeval Tethyan basins formed during the closure of the Paleotethys and early opening of the Neotethys.

Broader significance: These results establish the Çakrazboz Formation as a regional reference model for climate–hydrology interaction in Triassic lacustrine systems and provide a robust sedimentological record of continental responses to global climatic and tectonic reorganization during Pangea's fragmentation.

GENİŞLETİLMİŞ ÖZET

Batı Pontidler'in (Kuzeybatı Anadolu) Amasra–Kastamonu yöresinde yüzeylenen Çakrazboz Formasyonu, Türkiye'de bilinen tek Geç Triyas yaşlı kıtasal tortul istif olarak büyük önem taşımaktadır. Bu çalışmada, Çakraz, Bozköy, İncigez ve Başköy 1, 2 ve 3 olmak üzere toplam altı stratigrafik kesitte detaylı sedimantolojik, petrografik ve stratigrafik analizler gerçekleştirilmiş, formasyonun fasiyes mimarisi, çökelme ortamları ve iklimsel kontrol mekanizmaları ortaya konmuştur.

Saha gözlemleri ve ince kesit analizleri, formasyonun gölsel (lacustrine), bataklık (palustrine) ve akarsu (flüviyal) ortamlardan oluşan karmaşık bir fasiyes mozaiğine sahip olduğunu ortaya koymaktadır. Çakraz ve İncigez kesitlerindeki karbonatça zengin mikrit (çamurtaşı), vaketaşı ve istiftaşı mikrofasiyesleri düşük enerjili, derin göl–sublitoral ortamlarda çökelmiş olup, periyodik olarak anoksik koşulların etkili olduğunu göstermektedir. Bozköy ve Başköy-1 kesitlerinde gözlenen fenestral dokular, kök izleri, laminar kalkritler ve kuruma çatlakları ile karakterize pedojenik olarak değişmiş kireçtaşları ve marnlar, göl kenarı bataklıkları ve palüstrin ortamlarda tekrarlayan yüzeylenme ve yeniden taşkın döngülerini yansıtır. Başköy-2 ve Başköy-3 kesitleri ise, menderesli akarsu sistemlerine ait, yukarıya doğru incelen kumtaşı–çamurtaşı ardalanmaları ile temsil edilen nokta bar istiflerini barındırmaktadır.

Formasyondaki fasiyes dağılımı ve istiflenme desenleri, göl tipinin Bohacs ve ark. (2000)'daki dengeli dolgu (balanced-fill) modeli ile büyük oranda uyumlu olmakla birlikte, Zavala ve ark. (2024)'ın hidrolik göl sınıflandırmasına göre zaman içinde yetersiz dolu (underfilled), dengeli dolu (balanced-fill) ve aşırı dolu (overfilled) evreler arasında geçişlerin yaşandığını göstermektedir. Yetersiz dolu evreler, hidrolik olarak kapalı göllerde, karbonatça zengin profundal çökeller veya flüviyal–supratidal ardalanmalarla temsil

edilirken; dengeli dolu evreler, göl seviyesinin taşma kotuna ulaştığı, transgresif–regresif istiflerle tanımlanır. Aşırı dolu evrelerde ise sürekli tatlı su girişi, açık hidrolik sistemler oluşturmuş ve kalınlaşan–iri taneli progradasyonal deltalar ile temsil edilmiştir. Bu göl tipleri, iklim salınımlarına (özellikle presesyon ve eksantriklik döngülerine) yanıt olarak değişmiştir.

Paleoiklimsel değerlendirmeler, yeşilimsi gri marnların daha nemli, kırmızımsı kahverengi marnların ise daha kurak evrelere karşılık geldiğini göstermektedir. Bu renk değişimleri, pH ve Eh dalgalanmaları ile taban suyu seviyesindeki değişimlere bağlı oksidasyon–redüksiyon koşullarını yansıtır. Yüksek çözünürlüklü renk verileri, GSA Rock-Color Chart (2009) kullanılarak göl seviyesi ve oksijenlenme durumu ile ilişkilendirilmiştir. Ayrıca, göl tiplerindeki değişimin, havzanın sediman–su bütçesini kontrol eden iklim–hidroloji etkileşiminin doğrudan göstergesi olduğu sonucuna varılmıştır.

Sonuç olarak, Çakrazboz Formasyonu, göl tipi evrimleri ile iklimsel döngüler arasındaki ilişkiyi ortaya koyan, Geç Triyas iç havza sistemleri için önemli bir referans kesit niteliğindedir. Bulgular, Tetis kuşağındaki diğer Geç Triyas gölsel havzalarla karşılaştırmalara olanak sağlamaktadır.

ACKNOWLEDGMENT

This study is derived from the doctoral dissertation entitled “Sedimentological and Cyclostratigraphic Analysis of the Çakrazboz Formation (Triassic) in Amasra–Kastamonu Region”, conducted within the framework of the Council of Higher Education’s Faculty Member Training Program (ÖYP).

ORCID

Gül Şen https://orcid.org/0000-0002-9729-242X

İsmail Ömer Yılmaz https://orcid.org/0000-0002-7967-3026

REFERENCES

Adrian, R., O’Reilly, C. M., Zagarese, H., Baines, S. B., Hessen, D. O., Keller, W., ... & Winder, M. (2009). Lakes as sentinels of climate change. *Limnology and oceanography*, *54*(6 part 2), 2283-2297. https://doi.org/10.4319/lo.2009.54.6_part_2.2283

Akbaş, B., Altun, İ. T. & Bilgin, A. Z. (2002). *1:100,000 scale geological map of Turkey, Zonguldak E28 sheet*. General Directorate of Mineral Research and Exploration.

Akdoğan, R., Hu, X., Okay, A. I., Topuz, G. & Xue, W. (2021). Provenance of the Paleozoic to Mesozoic siliciclastic rocks of the İstanbul Zone constrains the timing of the Rheic Ocean closure in the Eastern Mediterranean region. *Tectonics*, *40*(12), e2021TC006824. https://doi.org/10.1029/2021TC006824

Akman, Ü. (1992). Amasra-Arıt arasının jeolojisi [Yayımlanmamış Doktora Tezi]. *PhD, Ankara University, Ankara, Turkey (in Turkish)*.

Alişan, C., Derman, A. S. (1995). The first palynological age, sedimentological and stratigraphic data for the Çakraz Group (Triassic), Western Black Sea. Erler, In A., Ercan, T., Bingöl, E., & Örçen, S. (Eds.), *Geology of the Black Sea region*, 93-98.

Alonso-Zarza, A. M. (2003). Palaeoenvironmental significance of palustrine carbonates and calcretes in the geological record. *Earth-Science Reviews*, *60*(3-4), 261–298. https://doi.org/10.1016/S0012-8252(02)00106-X

Alonso-Zarza, A. M. & Tanner, L. H. (2009). *Carbonates in continental settings: facies, environments, and processes*. Developments in Sedimentology, Volume 61. Elsevier.

Alonso-Zarza, A. M. & Wright, V. P. (2010). Palustrine carbonates. In A. M. Alonso-Zarza & L. H. Tanner (Eds.), *Developments in Sedimentology, 61*, (pp. 103–131). Elsevier. https://doi.org/10.1016/S0070-4571(09)06102-0

Argyilan, E. P. & Forman, S. L. (2003). Lake level response to seasonal climatic variability in the

Lake Michigan-Huron system from 1920 to 1995. *Journal of Great Lakes Research*, *29*(3), 488-500. https://doi.org/10.1016/S0380-1330(03)70453-5

Armenteros, I. (2010). Diagenesis of carbonates in continental settings. In Alonso-Zarza, A.M. & Tanner, L.H. (Eds.), *Developments in Sedimentology*, *62*, 61-151. https://doi.org/10.1016/S0070-4571(09)06202-5

Bathurst, R. G. (1987). Diagenetically enhanced bedding in argillaceous platform limestones: stratified cementation and selective compaction. *Sedimentology*, *34*(5), 749-778. https://doi.org/10.1111/j.1365-3091.1987.tb00801.x

Boggs Jr, S. (2014). *Principles of Sedimentology and Stratigraphy*. Pearson Education.

Boggs, S. (2006). *Principles of Sedimentology and Stratigraphy* (4th ed.). Pearson Prentice Hall.

Bohacs, K. M., Carroll, A. R., Neal, J. E., & Mankiewicz, P. J. (2000). Lake-basin type, source potential, and hydrocarbon character: An integrated sequence-stratigraphic–geochemical framework. In E. H. Gierlowski-Kordesch & K. R. Kelts (Eds.), *Lake Basins Through Space and Time*. (Vol. 3, pp. 3–34). AAPG Studies in Geology. https://doi.org/10.1306/St46706C1

Boucot, A. J., Xu, C., Scotese, C. R., & Morley, R. J. (2013). *Phanerozoic Paleoclimate: an Atlas of Lithologic Indicators of Climate* (vol. 11, pp. 1-30). SEPM (Society for Sedimentary Geology).

Bustillo, M. A., Armenteros, I., & Huerta, P. (2017). Dolomitization, gypsum calcitization and silicification in carbonate–evaporite shallow lacustrine deposits. *Sedimentology*, *64*(4), 1147-1172. https://doi.org/10.1111/sed.12345

Carroll, A. R., & Bohacs, K. M. (1999). Stratigraphic classification of ancient lakes: Balancing tectonic and climatic controls. *Geology*, 27(2), 99–102. https://doi.org/10.1130/0091-7613(1999)027<0099:SCOALB>2.3.CO;2

Cecil, C. B. (1990). Paleoclimate controls on stratigraphic repetition of chemical and siliciclastic rocks. *Geology*, *18*(6), 533–536. https://doi.org/10.1130/0091-7613(1990)018%3C0533:PCOSRO%3E2.3.CO;2

De Wet, C. B., Yocum, D. A. & Mora, C. I. (1998). Carbonate lakes in closed basins: sensitive indicators of climate and tectonics: an example from the Gettysburg Basin (Triassic), Pennsylvania, USA. In G. Kocurek (Ed.), *Relative Role of Eustacy, Climate, and Tectonism in Continental Rocks. SEPM Society for Sedimentary Geology.* https://doi.org/10.2110/pec.98.59.0191

Dickinson, W. R. (1985). Interpreting provenance relations from detrital modes of sandstones. In: Zuffa, G. G. (Eds.), *Provenance of Arenites*, (Series C, 148, pp. 333-361). North Atlantic Treaty Organization - Advanced Study Institutes (NATO-ASI). https://doi.org/10.1007/978-94-017-2809-6_15

Dobkins, J. E. & Folk, R. L. (1970). Shape development on Tahiti-nui. *Journal of Sedimentary Research*, *40*(4), 1167-1203. https://doi.org/10.1306/74D72162-2B21-11D7-8648000102C1865D

Dunham, R. J. (1962). Classification of carbonate rocks according to depositional texture. In W. E. Ham (Ed.), *Classification of Carbonate Rocks*, (pp. 108–121). AAPG Memoir 1.

Fijałkowska-Mader, A., Heunisch, C. & Szulc, J. (2015). Palynostratigraphy and palynofacies of the Upper Silesian Keuper (southern Poland). *Annales Societatis Geologorum Poloniae*, 85(4), 637-661. https://doi.org/10.14241/asgp.2015.025

Flügel, E. (2010). *Microfacies of Carbonate Rocks: Analysis, Interpretation and Application* (2nd ed.). Springer.

Folk, R. L. (1959). Practical petrographic classification of limestones. *AAPG Bulletin*, 43(1), 1–38. https://doi.org/10.1306/0BDA5C36-16BD-11D7-8645000102C1865D

Folk, R. L. & Ward, W. C. (1957). Brazos River bar [Texas]; a study in the significance of grain size

parameters. *Journal of Sedimentary Research*, *27*(1), 3-26. https://doi.org/10.1306/74D70646-2B21-11D7-8648000102C1865D

Franke, W., Paul, J. (1980). Pelagic redbeds in the Devonian of Germany – deposition and diagenesis. *Sedimentary Geology*, 25(3), 231–256. https://doi.org/10.1016/0037-0738(80)90043-3

Freytet, P. (1973). Petrography and paleo-environment of continental carbonate deposits with particular reference to the Upper Cretaceous and Lower Eocene of Languedoc (Southern France). *Sedimentary Geology*, *10*(1), 25-60. https://doi.org/10.1016/0037-0738(73)90009-2

Freytet, P. & Verrecchia, E.P. (2002). Lacustrine and palustrine carbonate petrography: an overview. *Journal of Paleolimnology, 27*, 221–237. https://doi.org/10.1023/A:1014263722766

Friedman, G. M. (1961). Distinction between dune, beach and river sands from their textural characteristics. *Journal of Sedimentary Petrology, 31*(4), 514-529. https://doi.org/10.1306/74D70BCD-2B21-11D7-8648000102C1865D

Gamero-Diaz, H., Miller, C. & Lewis, R. (2012). sCore: a classification scheme for organic mudstones based on bulk mineralogy. *Search and Discovery,* Article *40951*.

Gand, G., Tüysüz, O., Steyer, J. S., Allain, R., Sakınç, M., Sanchez, S., Şengör, A. M. C, & Sen, S. (2011). New Permian tetrapod footprints and macroflora from Turkey (Çakraz Formation, northwestern Anatolia): Biostratigraphic and palaeoenvironmental implications. *Comptes Rendus Palevol, 10*(8), 617-625. https://doi.org/10.1016/j.crpv.2011.09.002

Gedik, I. & Aksay, A. (2002). *1:100,000 scale geological map of Turkey, Zonguldak E29 sheet*. General Directorate of Mineral Research and Exploration.

Geological Society of America (GSA). (2009). *Rock-Color Chart*. Geological Society of America.

Gierlowski-Kordesch, E. H. (2010). Lacustrine carbonates. In A. M. Alonso-Zarza & L. H. Tanner (Eds.), *Carbonates in Continental Settings: Facies, Environments and Processes,* (Vol. 61, pp. 1–101). Elsevier. https://doi.org/10.1016/S0070-4571(09)06101-9

Glenn, C. R. & Kelts, K. (1991). Sedimentary rhythms in lake deposits. *Cycles and Events in Stratigraphy*, (pp. 188–221). Springer.

Golonka, J. (2007). Late Triassic and Early Jurassic palaeogeography of the world. *Palaeogeography, Palaeoclimatology, Palaeoecology*, *244*(1-4), 297-307. https://doi.org/10.1016/j.palaeo.2006.06.041

Gvirtzman, G. (2006). Groundwater hydrology and paleohydrology of the Dead Sea rift valley, In Y. Enzel, A. Agnon, M. Stein (Eds.), *New Frontiers in Dead Sea Paleoenvironmental Research*. *Geological Society of America*. https://doi.org/10.1130/2006.2401(06)

Haq, B. U., Hardenbol, J. A. N., & Vail, P. R. (1987). Chronology of fluctuating sea levels since the Triassic. *Science*, *235*(4793), 1156-1167. https://doi.org/10.1126/science.235.4793.1156

Hedges, J. I., & Stern, J. H. (1984). Carbon and nitrogen determinations of carbonate-containing solids. *Limnology and Oceanography*, *29*(3), 657-663. https://doi.org/10.4319/lo.1984.29.3.0657

Immenhauser, A. (2022). On the delimitation of the carbonate burial realm. *The Depositional Record*, *8*(2), 524-574. https://doi.org/10.1002/dep2.173

Kürschner, W. M. & Herngreen, G. W. (2010). Triassic palynology of central and northwestern Europe: a review of palynofloral diversity patterns and biostratigraphic subdivisions. In S.G. Lucas (Ed.), *The Triassic Timescale*, (pp. 263-283). The Geological Society of London. https://doi.org/10.1144/SP334.11

Kutzbach, J. E. (1994). Idealized Pangean climates: sensitivity to orbital change. In G. O. Klein (Ed.), *Pangea: Paleoclimate, Tectonics, and Sedimentation During Accretion, Zenith, and*

Breakup of a Supercontinent. Geological Society of America. https://doi.org/10.1130/SPE288-p41

Mattes, B. W., & Mountjoy, E. W. (1980). Burial dolomitization of the Upper Devonian Miette buildup, Jasper National Park, Alberta. *The Society of Economic Paleontologists and Mineralogist*s, 28, 259-297. https://archives.datapages.com/data/sepm_sp/SP28/Burial_Dolomitization.htm

Miall, A. D. (1996). *The Geology of Fluvial Deposits: Sedimentary Facies, Basin Analysis, and Petroleum Geology.* Springer-Verlag. https://doi.org/10.1007/978-3-662-03237-4

Moiola, R. J. & Weiser, D. (1968). Textural parameters: An evaluation. *Journal of Sedimentary Petrology, 38,* 45-53. https://doi.org/10.1306/74D718C5-2B21-11D7-8648000102C1865D

Montañez, I. P. & Crossey, L. J. (1998). Diagenesis of sedimentary rocks. In G. N. Hanson (Ed.), *Encyclopedia of Earth Sciences*, (pp. 145–160). Springer.

Moore, C. H. (1989). *Carbonate Diagenesis and Porosity*. Elsevier.

Moore, C. H. & Wade, W. J. (2013). *Carbonate Reservoirs: Porosity and Diagenesis in a Sequence Stratigraphic Framework* (2nd ed.). Elsevier.

Nikishin, A. M., Okay, A. I., Tüysüz, O., Demirer, A., Amelin, N. & Petrov, E. (2015a). The Black Sea basins structure and history: New model based on new deep penetration regional seismic data. Part 1: Basins structure and fill. *Marine and Petroleum Geology*, *59*, 638-655. https://doi.org/10.1016/j.marpetgeo.2014.08.017

Nikishin, A. M., Okay, A., Tüysüz, O., Demirer, A., Wannier, M., Amelin, N. & Petrov, E. (2015b). The Black Sea basins structure and history: New model based on new deep penetration regional seismic data. Part 2: Tectonic history and paleogeography. *Marine and Petroleum Geology*, *59*, 656-670. https://doi.org/10.1016/j.marpetgeo.2014.08.018

Okay, A. I. & Nikishin, A. M. (2015). Tectonic evolution of the southern margin of Laurasia in the Black Sea region. *International Geology Review*, *57*(5-8), 1051-1076. https://doi.org/10.1080/00206814.2015.1010609

Okay, A. I. & Tüysüz, O. (1999). Tethyan sutures of northern Turkey. In B. Durand et al. (Eds.), *The Mediterranean Basins: Tertiary Extension within the Alpine Orogen* (pp. 475–515). Geological Society of London. https://doi.org/10.1144/GSL.SP.1999.156.01.22

Passega, R. (1964). Grain size characteristics by C-M pattern as a tool. *Journal of Sedimentary Petrology, 34,* 233-847. https://doi.org/10.1306/74D711A4-2B21-11D7-8648000102C1865D

Pettijohn, F. J., Potter, P. E. & Siever, R. (1973). *Sand and Sandstone*. Springer.

Pettijohn, F. J., Potter, P. E. & Siever, R. (2012). *Sand and Sandstone.* Springer Science & Business Media.

Pettijohn, F.J., Potter, P. E. & Siever, R. (1987). *Sand and Sandstone* (2nd ed.). Springer-Verlag.

Philcox, M. E. (1963). Banded calcite mudstone in the lower Carboniferous" reef" knolls of the Dublin Basin, Ireland. *Journal of Sedimentary Research*, *33*(4), 904-913. https://doi.org/10.1306/74D70F6F-2B21-11D7-8648000102C1865D

Platt, N. H., & Wright, V. P. (1992). Palustrine carbonates and the Florida Everglades; towards an exposure index for the fresh-water environment?. *Journal of Sedimentary Research*, *62*(6), 1058-1071. https://doi.org/10.1306/D4267A4B-2B26-11D7-8648000102C1865D

Powers, M. C. (1953). A new roundness scale for sedimentary particles. *Journal of Sedimentary Research*, *23*(2), 117-119. https://doi.org/10.1306/D4269567-2B26-11D7-8648000102C1865D

Rafferty, J. P. (Ed.). (2010). *Climate and Climate Change*. Britannica Educational Publishing.

Raynaud, D., Jouzel, J., Barnola, J. M., Chappellaz, J., Delmas, R. J., & Lorius, C. (1993). The ice record of greenhouse gases. *Science*, 926-934. https://doi.org/10.1126/science.259.5097.926

Reading, H. G. & Levell, B. K. (1996). Controls on the sedimentary rock record. In H. G. Reading (Ed.), *Sedimentary Environments: Processes, Facies and Stratigraphy,* (3rd ed.). Blackwell Science.

Rech-Frollo, M. (1971). Les calcaires des couches rouges des alpes: Leur composition et leur origine. *Sedimentary Geology*, *6*(1), 53-72. https://doi.org/10.1016/0037-0738(71)90026-1

Reineck, H. E. & Singh, I. B., (1980). *Depositional Sedimentary Environments*. Springer. https://doi.org/10.1007/978-3-642-81498-3

Robertson, A. H. F., Parlak, O. & Ustaömer, T. (2016). Permian–Recent palaeogeographical and tectonic development of Anatolia: Some recent contributions. *International Journal of Earth Sciences*, 105, 1–5. https://doi.org/10.1007/s00531-015-1247-2

Robinson, A. G. (Ed.). (1997). *Regional and Petroleum Geology of the Black Sea and Surrounding Region.* AAPG Memoir, 68. https://doi.org/10.1306/M68612

Rutherford, M. M., Banks, C., Hirst, P. P. & Robinson, A. G. (1992). The *Mesozoic biostratigraphy of the Pontides*. Unpublished Internal Report, BP Exploration, Middlesex, UK., 9 p.

Sames, B., Wagreich, M., Conrad, C. P. & Iqbal, S. (2020). Aquifer-eustasy as the main driver of short-term sea-level fluctuations during Cretaceous hothouse climate phases. *Geological Society of London Special Publications 498,* 9-38. https://doi.org/10.1144/SP498-2019-105

Schettino, A., & Turco, E. (2011). Tectonic history of the western Tethys since the Late Triassic. *GSA Bulletin, 123*(1–2), 89–105. https://doi.org/10.1130/B30064.1

Scotese, C. R. & Schettino, A. (2017). Late Permian–Early Jurassic paleogeography of western Tethys and the world. *Permo-Triassic Salt Provinces of Europe, North Africa and the Atlantic Margins, Tectonics and Hydrocarbon Potential.* Elsevier. https://doi.org/10.1016/B978-0-12-809417-4.00004-5

Scotese, C. R. (2021). An atlas of Phanerozoic paleogeographic maps: the seas come in and the seas go out. *Annual Review of Earth and Planetary Sciences*, *49*(1), 679-728. https://doi.org/10.1146/annurev-earth-081320-064052

Scotese, C. R., Bambach, R. K., Barton, C., Van der Voo, R. & Ziegler, A. M. (1979). Paleozoic base maps *The Journal of Geology 87*(3), 217-277.

Şen, G. (2021). *Sedimentological and cyclostratigraphic analysis of the Çakrazboz Formation (Triassic) in Amasra-Kastamonu Region* [Published PhD Dissertation]. Middle East Technical University Graduate School of Natural and Applied Sciences.

Şengör, A. M. C. (1979). Mid-Mesozoic closure of Permo–Triassic Tethys and its implications. *Nature*, *279*(14), 590-593. https://doi.org/10.1038/279590a0

Şengör, A. M. C. (Ed.) (1989). *Tectonic evolution of the Tethyan region*. Nato Science Series C, Springer. https://doi.org/10.1007/978-94-009-2253-2

Şengör, A. M. C. (1990). Plate tectonics and orogenic research after 25 years: A Tethyan perspective. *Earth-Science Reviews*, *27*(1-2), 1-201. https://doi.org/10.1016/0012-8252(90)90002-D

Simmons, M. D., Tari, G. C. & Okay, A. I. (2018). Petroleum geology of the Black Sea: introduction. *Geological Society, London, Special Publications*, *464*(1), 1-18. https://doi.org/10.1144/SP464.15

Sneed, E. D. & Folk, R. L. (1958). Pebbles in the lower Colorado River, Texas a study in particle morphogenesis. *The Journal of Geology*, *66*(2), 114-150. https://www.jstor.org/stable/30058239

Stewart, H. B. Jr. (1958). Sedimentary reflections on depositional environments in San Migue Lagoon, Baja California, Mexico. *Bulletin of the American Association of Petroleum Geologists, (42)* 2567-2618. https://doi.org/10.1306/0BDA5BFA-16BD-11D7-8645000102C1865D

Stolle, E. (2016). Çakraz Formation, Çamdağ area, NW Turkey: Early/mid-Permian age, Rotliegend (Germany) and Southern Alps (Italy) equivalent - a stratigraphic re-assessment via palynological

long-distance correlation. *Geological Journal, 51*(2), 223-235. https://doi.org/10.1002/gj.2620

Stow, D. A. (2005). *Sedimentary Rocks in the Field: A color guide*. Gulf Professional Publishing.

Swart, P. K. (2015). The geochemistry of carbonate diagenesis: The past and future. *Sedimentology*, 62(6), 1233–1304. https://doi.org/10.1111/sed.12205

Tucker, M. E. (1990). Diagenetic processes, products and environments. In M. E. Tucker & V. P. Wright (Eds.), *Carbonate Sedimentology*, (pp. 314–364). John Wiley & Sons. https://doi.org/10.1002/9781444314175.ch7

Tucker, M. E. & Bathurst, R. G. (Eds.). (1990). *Carbonate Diagenesis*. John Wiley & Sons. https://doi.org/10.1002/9781444304510

Tucker, M. E. & Sparks, R. S. J. (2024). Fluvial–lacustrine interactions in the Marginal Triassic, Clevedon, Bristol Channel Basin, UK: Deposition, dolomitization and silicification. *Geological Magazine, 161*(e18). https://doi.org/10.1017/S0016756824000396

Tucker, M. E. & Wright, V. P. (1990). *Carbonate Sedimentology*. Blackwell. https://doi.org/10.1002/9781444314175

Tüysüz, O. (2022). Geology of the Kurucaşile-Cide region, NW Türkiye. *Bulletin of the Mineral Research and Exploration*, *167*(167), 149-178.

Van Hinsbergen, D. J., Torsvik, T. H., Schmid, S. M., Maţenco, L. C., Maffione, M., Vissers, R. L., ... & Spakman, W. (2020). Orogenic architecture of the Mediterranean region and kinematic reconstruction of its tectonic evolution since the Triassic. *Gondwana Research*, 81, 79-229. https://doi.org/10.1016/j.gr.2019.07.009

Varol, B. & Akman, N. (1988). *Geological map of the Amasra–Çakraz area, (No. 42)*. MTA.

Verardo, D. J., Froelich, P. N. & McIntyre, A., (1990). Determination of organic carbon and nitrogen in marine sediments using the Carlo Erba NA-1500 Analyzer. *Deep Sea Research Part A. Oceanographic Research Papers*, *37*(1), 157-165. https://doi.org/10.1016/0198-0149(90)90034-S

Verrecchia, E. P. (2000). Fungi and sediments. In Riding, R. E. & Awramik, S.M. (Eds.) *Microbial sediments.* Springer Berlin Heidelberg. https://doi.org/10.1007/978-3-662-04036-2_9

Verrecchia, E. P. (2007). Lacustrine and palustrine geochemical sediments. In *Geochemical Sediments and Landscapes* (pp. 298-329). Blackwell Publishing Oxford. https://doi.org/10.1002/9780470712917.ch9

Vollmer, T., Werner, R., Weber, M., Tougiannidis, N., Röhling, H. G. & Hambach, U. (2008). Orbital control on Upper Triassic Playa cycles of the Steinmergel-Keuper (Norian): A new concept for ancient playa cycles. *Palaeogeography, Palaeoclimatology, Palaeoecology, 267*(1-2), 1-16. https://doi.org/10.1016/j.palaeo.2007.12.017

Wagreich, M., Lein, R. & Sames, B. (2014). Eustasy, its controlling factors, and the limno-eustatic hypothesis–concepts inspired by Eduard Suess. *Austrian Journal of Earth Sciences*, *107*(1), 115-131.

Wang, Y., Sheng, H. F., He, Y., Wu, J. Y., Jiang, Y. X., Tam, N. F. Y. & Zhou, H. W. (2012). Comparison of the levels of bacterial diversity in freshwater, intertidal wetland, and marine sediments by using millions of illumina tags. *Applied and Environmental Microbiology*, *78*(23), 8264-8271. https://doi.org/10.1128/aem.01821-12

Wright, V. P. (2009). Meteoric diagenesis. In M. E. Tucker & V. P. Wright (Eds.), *Carbonate Sedimentology,* (pp. 336–348). John Wiley & Sons.

Wright, V. P., & Tucker, M. E. (1991). *Calcretes*. Blackwell Scientific Publications. https://doi.org/10.1002/9781444304497

Yilmaz, Y., Tüysüz, O., Yiğitbaş, E., Genç, Ş. C. & Şengor, A. M. C. (1997). Geology and tectonic evolution of the Pontides. In A. G. Robinson (Ed.), Regional and Petroleum Geology of the Black Sea and Surrounding Region.

American Association of Petroleum Geologists. https://doi.org/10.1306/M68612C11

Yılmazer, S., Topuz, G., Guillong, M., Okay, A. I., Demirkaya, İ. & Uzun, F. (2025). Revealing the early geological history of the İstanbul Zone (Far-East Avalonia) through zircon U-Pb-Hf isotopic data. *Precambrian Research*, *427*, Article107855. https://doi.org/10.1016/j.precamres.2025.107855

Zavala, C., Liu, H.-Q., Li, X.-B., Trobbiani, V., Li, Y., Arcuri, M. & Zorzano, A. (2024). High-frequency lacustrine sequence stratigraphy of clastic lakes: Lessons from ancient successions. *Journal of Palaeogeography, 13*(4), 621–645. https://doi.org/10.1016/j.jop.2024.08.004.

Zielinski, G. A., Germani, M. S., Larsen, G., Baillie, M. G., Whitlow, S., Twickler, M. S. & Taylor, K. (1995). Evidence of the Eldgjá (Iceland) eruption in the GISP2 Greenland ice core: relationship to eruption processes and climatic conditions in the tenth century. *The Holocene*, *5*(2), 129-140. https://doi.org/10.1177/095968369500500201